

<b>1</b>	<b>Iron-Carbon Alloys I</b>	<b>1</b>
1-1	Elemental Iron	2
1-2	The Fe-Fe <sub>3</sub> C Alloy System	3
	Fe-Fe <sub>3</sub> C Phase Diagram / Solid Phases in the Fe-Fe <sub>3</sub> C Phase Diagram / Invariant Reactions in the Fe-Fe <sub>3</sub> C Phase Diagram / Critical Temperatures / Eutectoid, Hypoeutectoid, and Hypereutectoid Plain-Carbon Steels	
1-3	Slow Cooling of Plain-Carbon Steels	8
	Eutectoid Plain-Carbon Steels / Hypoeutectoid Plain-Carbon Steels / Hypereutectoid Plain-Carbon Steels	
1-4	Isothermal Transformation of an Eutectoid Plain-Carbon Steel	14
1-5	Transformation of Austenite to Pearlite	17
	Mechanism and Morphology / Effects of Temperature / Effects of Grain Size / The Strength of Pearlite	
1-6	Transformation of Austenite to Martensite	26
	Characteristics of the Martensitic Transformation in Plain-Carbon Steels / The Morphology of Martensite in Fe-C Alloys / Mechanism of Formation of Martensite in Plain-Carbon Steels / Kinetics of Formation of Martensite in Plain-Carbon Steels / Strength and Hardness of Martensite in Fe-C Alloys	
	Problems	41

---

# CHAPTER 1

---

## IRON-CARBON ALLOYS I

Iron is by far the least expensive of all the metals and, next to aluminum, the most plentiful. Iron and its many alloys constitute about 90 percent of the world's production of metals. Pure iron itself is used only for a relatively few special applications. Most iron is used in the form of *plain-carbon steels*, which are alloys of iron and carbon with small amounts of other elements.

In 1988, the United States produced 99.9 million tons of steel.<sup>1</sup> Plain-carbon steels accounted for 77.7 percent of this production. The reasons for the importance of plain-carbon steels is that they are strong, tough, ductile, and *inexpensive* materials that can be cast, worked, machined, and heat-treated to a wide range of properties. Unfortunately, plain-carbon steel has poor atmospheric corrosion resistance. But it can easily be protected by painting, enameling, or galvanizing. No other engineering material offers such a desirable combination of properties at such a low cost as does plain-carbon steel. Indeed, basically speaking, the highly industrialized countries of the world are still living in an "iron age," and will continue to do so into the foreseeable future.

In this book on engineering alloys, iron and steel topics constitute over half of the subject matter, which is justified in view of the importance of ferrous alloys. In Chaps. 1 and 2, iron-carbon (Fe-C) alloys are treated from a fundamental standpoint of their structure and heat treatment. Chapter 3 deals with the structure and properties of plain-carbon steels, and Chap. 4 with alloy

---

<sup>1</sup>"1988 Annual Statistical Report," American Iron and Steel Institute, Washington, D.C., 1989.

tonnes  $\times 10^6$

1200

1000

800

600

400

200

0

1900

1920

1940

1960

1980

2000

Year

2004

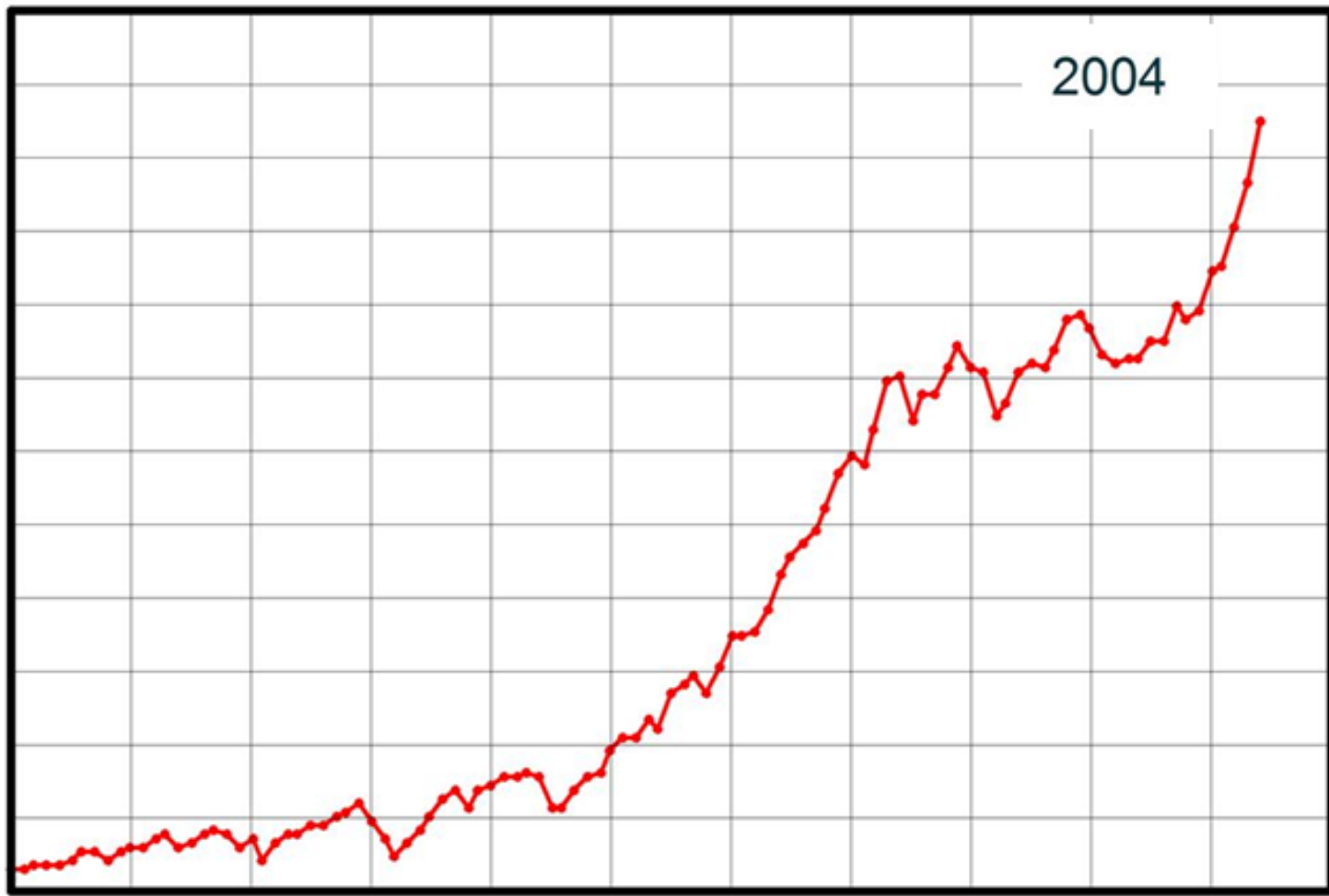


**TABLE 1-1**  
**Mechanical properties of some fully annealed irons at 21°C†**

Type of iron	Tensile strength, psi	Yield strength, psi	Elongation, %
Zone-refined iron	28,000	7,000	
Electrolytic iron (vacuum melted)	35,000–40,000	10,000–20,000	40–60
Ingot iron (Armco)	41,000	18,000	47

† Data from *Metals Handbook*, vol. I: "Properties," p. 211, American Society for Metals, Metals Park, Ohio, 1961.

steels. Other groups of ferrous alloys such as stainless steels, cast irons, and tool steels are dealt with in Chaps. 7, 8, and 9, respectively.

## 1-1 ELEMENTAL IRON

Very pure iron is produced only in small quantities and is used principally for research purposes. By zone refining, it can be made more than 99.99 percent pure. The yield strength of this pure iron is very low, being about 7500 psi (Table 1-1). Slightly less pure iron (99.9 percent) is produced commercially and has a higher yield strength (10,000 to 20,000 psi). Small quantities of elements such as carbon, manganese, phosphorus, and sulfur produce this great increase in the strength of elemental iron. The mechanical properties of some fully annealed irons are listed in Table 1-1, while their chemical compositions are given in Table 1-2.

Pure iron exists in three allotropic forms: alpha ( $\alpha$ ), gamma ( $\gamma$ ), and delta ( $\delta$ ). Figure 1-1 shows an idealized cooling curve for pure iron, indicating the temperature ranges over which each of these crystallographic forms are stable at atmospheric pressure. From room temperature to 910°C, pure iron has a body-centered cubic (BCC) crystal structure, and is called  $\alpha$  iron.  $\alpha$  iron is ferromagnetic, but on heating to 768°C (Curie point), the ferromagnetism disappears but the crystal structure remains BCC. Nonferromagnetic  $\alpha$  iron is

**TABLE 1-2**  
**Chemical compositions of some relatively pure irons**

Type of iron	Chemical composition, %								
	C	Mn	P	S	Si	Cu	Ni	O <sub>2</sub>	N <sub>2</sub>
Armco ingot iron	0.012	0.017	0.005	0.025	trace	...	...	...	...
Electrolytic	0.006	...	0.005	0.004	0.005	...	...	...	...
H <sub>2</sub> purified	0.005	0.028	0.004	0.003	0.0012	...	...	0.003	0.0001



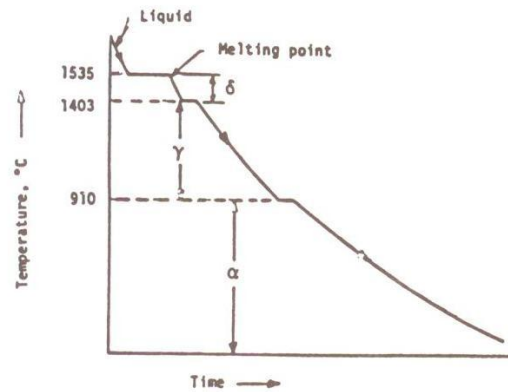


**FIGURE 1-1**  
Idealized cooling curve for pure iron  
at atmospheric pressure.

**TABLE 1-3**  
Crystallographic properties of pure iron

Allotropic forms	Crystallographic form	Unit cube edge, Å	Temperature range
Alpha	BCC	2.86(70°F)	Up to 910°C(1670°F)
Gamma	FCC	3.65(1800°F)	910–1403°C(1670–2557°F)
Delta	BCC	2.93(2650°F)	1403–1535°C(2557–2795°F)
Density, 7.868 g/cm <sup>3</sup>	Melting point, 1535°C(2795°F)		Boiling point, 3000°C(5432°F)

stable up to 910°C and then is transformed into face-centered cubic (FCC)  $\gamma$  iron. Upon heating to 1403°C, the  $\gamma$  iron is transformed back again into the BCC structure as  $\delta$  iron, which is stable up to the melting point of pure iron, 1535°C. The high-temperature BCC iron has a longer cube edge than BCC  $\alpha$  iron. Table 1-3 summarizes the crystallographic properties of pure iron.

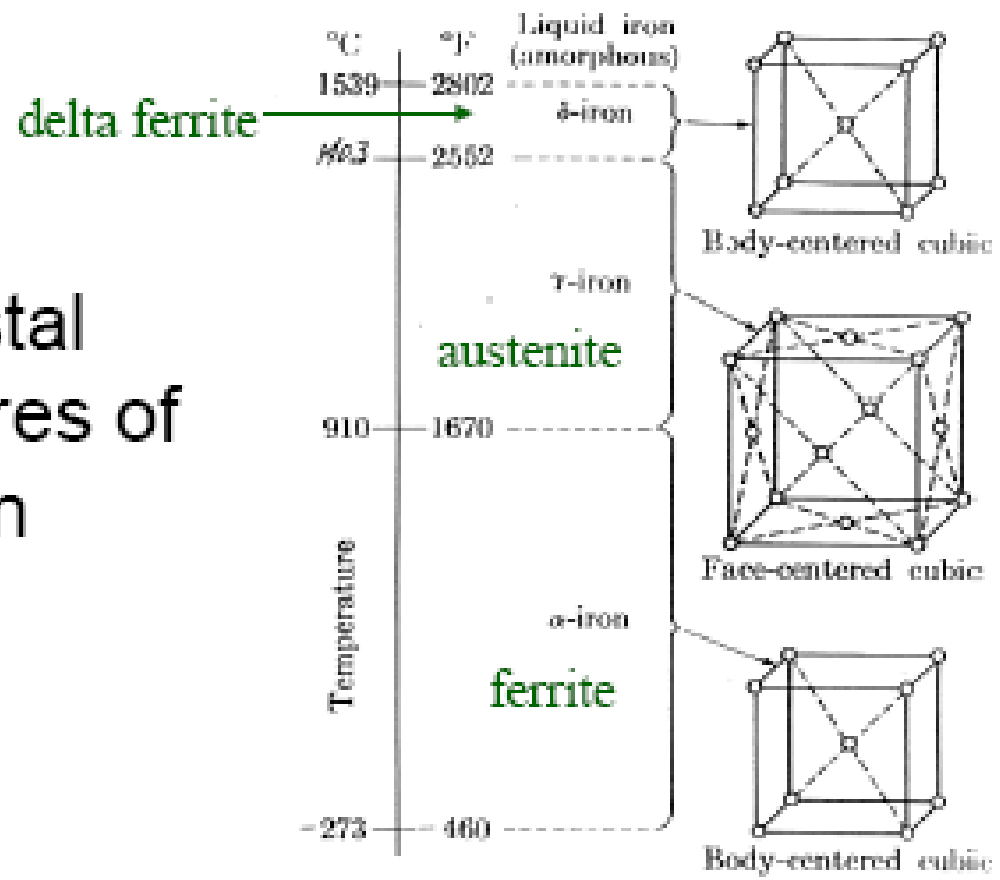
## 1-2 THE Fe-Fe<sub>3</sub>C ALLOY SYSTEM

Fe-C alloys containing from a trace to about 1.2% carbon (abbreviated “1.2% C”) and with only minor amounts of other elements are termed *plain-carbon steels*. However, for purposes of this first chapter the plain-carbon steels will be treated as essentially binary Fe-C alloys. The effects of other alloying elements and impurities will be discussed in subsequent chapters.

### Fe-Fe<sub>3</sub>C Phase Diagram

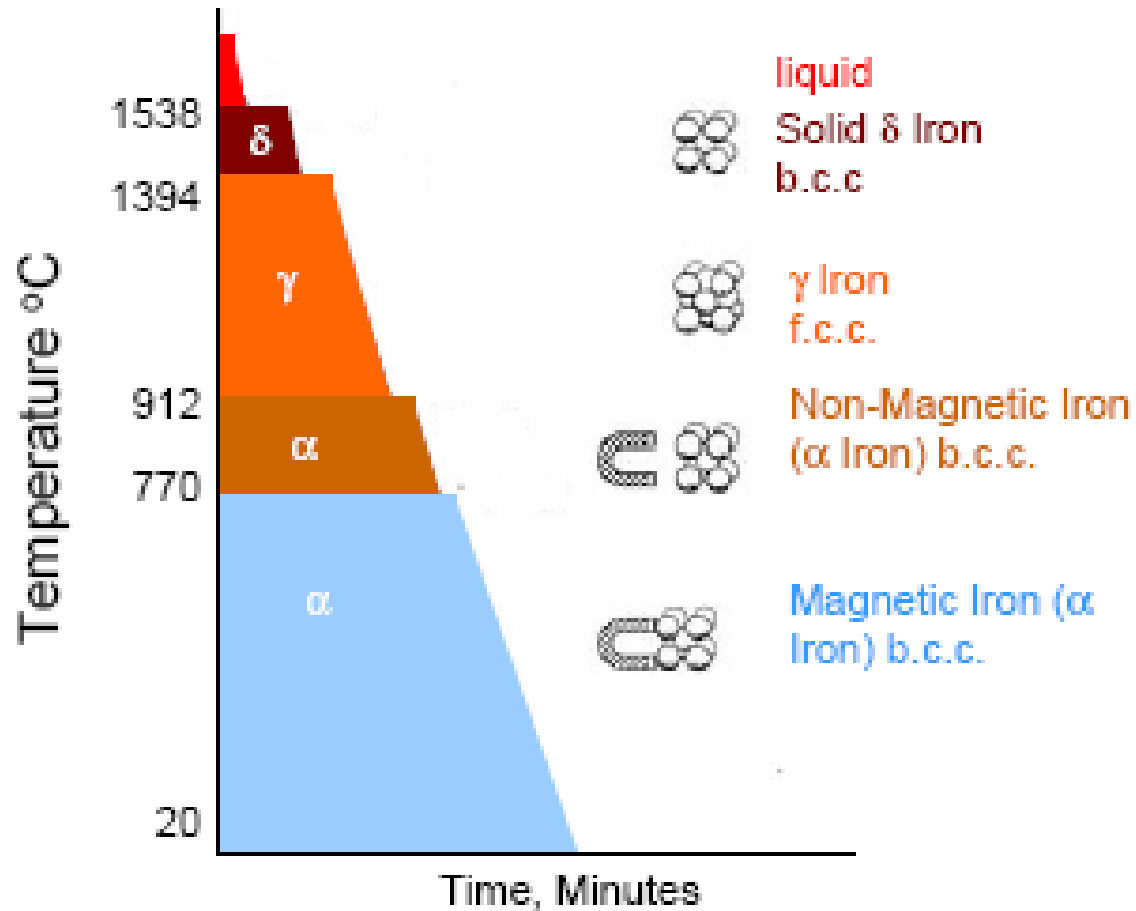
The phases present at various temperatures for very slowly cooled Fe-C alloys with up to 6.67% C are shown in the phase diagram of Fig. 1-2. This phase

# Crystal structures of iron



The temperature ranges in which the allotropic forms of iron exist under equilibrium conditions.

# Crystal structures of iron



# Introduction to Fe-C phase diagram

- Regions:

- Steels  $0 < \text{wt}\% \text{C} < 2$

- Cast iron  $2 < \text{wt}\% \text{C} < 4$   $1 < \text{wt}\% \text{Si} < 3$

- Phases:

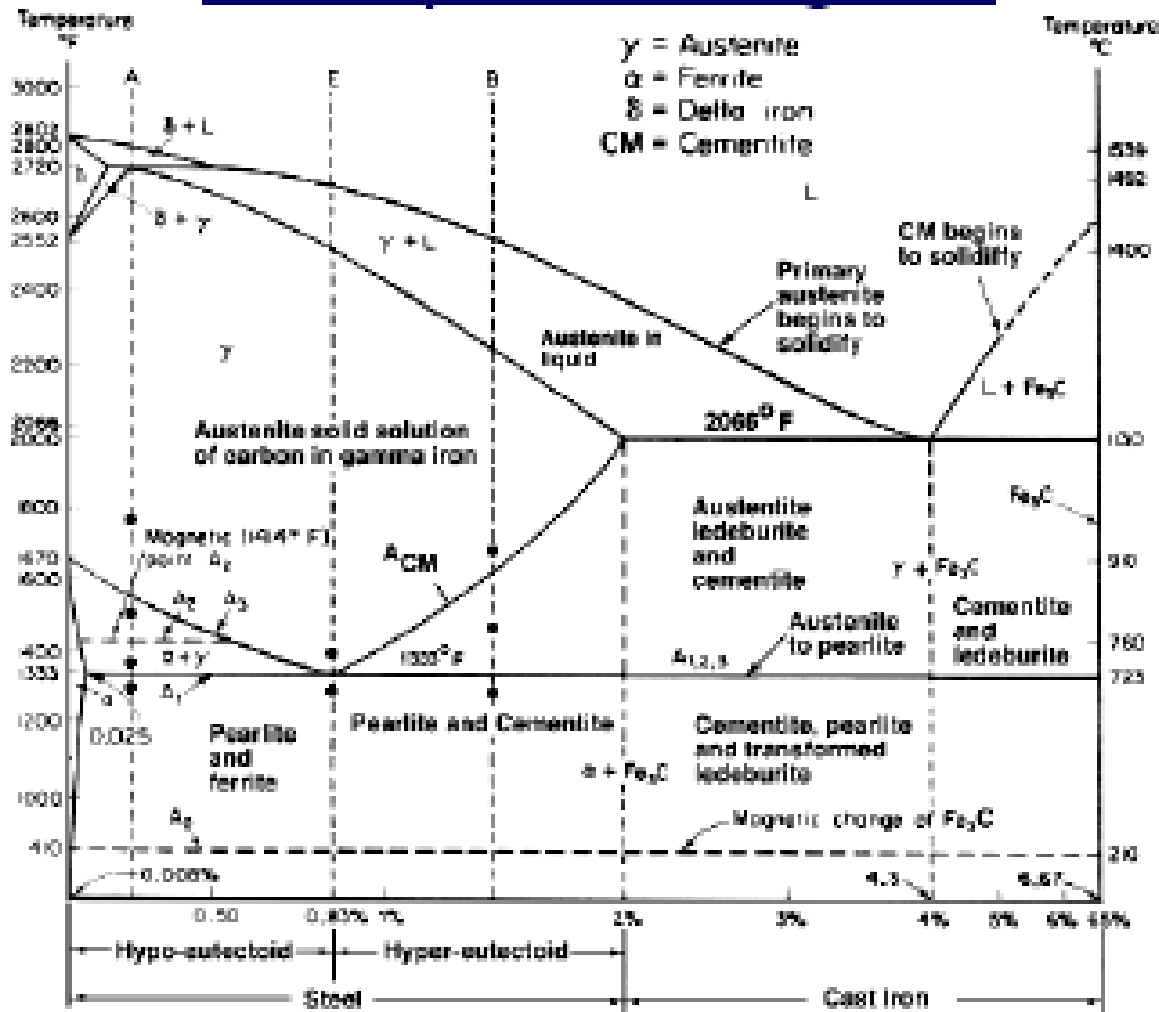
- Ferrite

- Austenite

- Cementite



# Fe-C phase diagram



# Four solid phases

- **$\alpha$ -ferrite**
  - solid solution of carbon in  $\alpha$ -iron,
  - BCC structure
  - carbon only slightly soluble in the matrix
    - maximum solubility of 0.02%C at 723°C to about 0.008%C at room temperature.
- **Austenite ( $\gamma$ )**
  - solid solution of carbon in  $\gamma$ -iron
  - FCC structure: can accommodate more carbon than ferrite
    - maximum of 2.08%C at 1148°C, decreases to 0.8%C at 723°C
    - difference in C solid solubility between  $\gamma$  and  $\alpha$  is the basis for **hardening** of most steels.

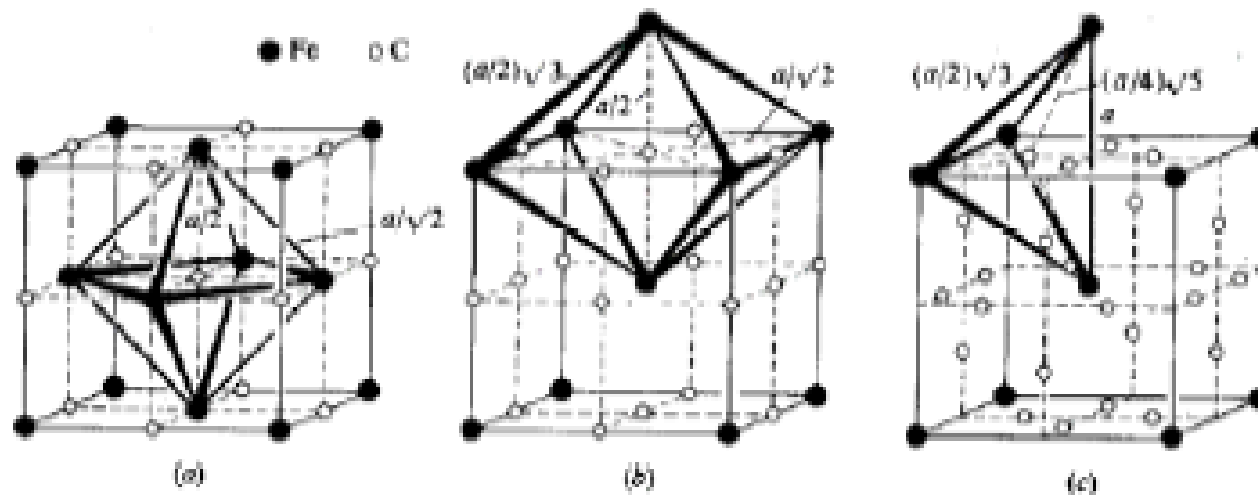
## **$\delta$ -ferrite**

- solid solution of carbon in  $\delta$ -iron
- BCC crystal structure
  - maximum solubility of ferrite being 0.09%C at 1495°C

- **Cementite ( $\text{Fe}_3\text{C}$ )**

- intermetallic Fe-C compound
  - $\text{Fe}_3\text{C}$  : 6.67%C and 93.3%Fe.
- orthorhombic crystal structure: hard and brittle

## Solubility of carbon:



- $\gamma$  fcc- iron: higher C solubility (a)
- $\alpha$  bcc-iron: lower C solubility (b, c)



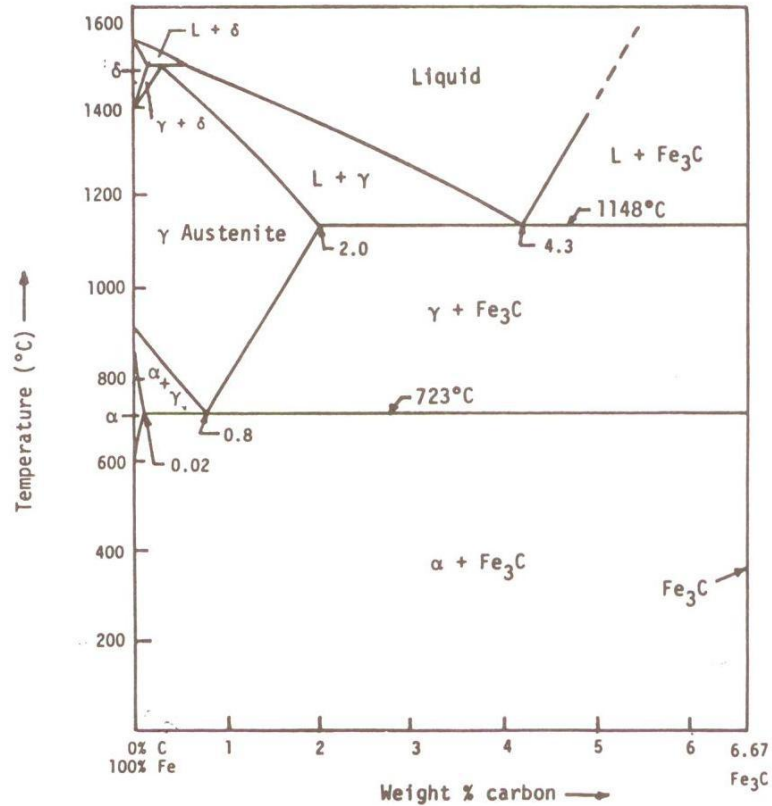


**FIGURE 1-2**  
The Fe-Fe<sub>3</sub>C metastable system. In this binary system, there are three important invariant reactions: peritectic at 1495°C, eutectic at 1148°C, and eutectoid at 723°C.

diagram is not a true equilibrium diagram since the intermetallic compound iron carbide (Fe<sub>3</sub>C), or *cementite* as it is called, is not a true equilibrium phase. Under certain conditions cementite will decompose into the more stable phases of graphite and iron. However, once Fe<sub>3</sub>C is formed, it is for all practical purposes very stable and therefore can be treated as an “equilibrium” phase. For this reason, the phase diagram shown in Fig. 1-2 is a metastable phase diagram.

### Solid Phases in the Fe-Fe<sub>3</sub>C Phase Diagram

The Fe-Fe<sub>3</sub>C phase diagram (Fig. 1-2) contains four solid phases: α ferrite, austenite, cementite (Fe<sub>3</sub>C), and δ ferrite. A description of each of these phases follows.

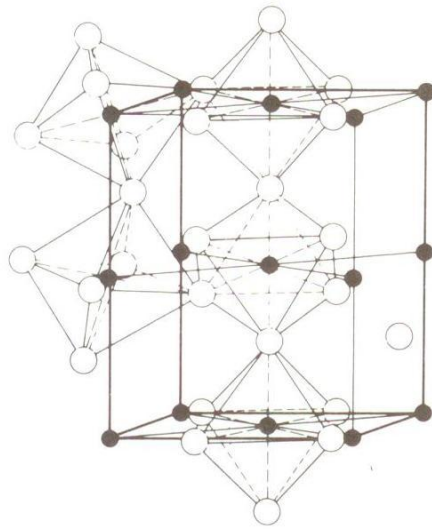


**FIGURE 1-3**

The atomic structure of cementite ( $\text{Fe}_3\text{C}$ ). Iron carbide ( $\text{Fe}_3\text{C}$ ) has an orthorhombic unit cell consisting of 12 iron atoms and 4 carbon atoms. Positions of the carbon atoms are indicated by the solid circles and those of the iron atoms by open circles. (After S. B. Hendricks, *Zeit. Kristal.* 74 (1930) 534, as shown in "The Making, Shaping and Treating of Steel," 9th ed., United States Steel Co., 1971, p. 1077.)

**$\alpha$  FERRITE.** The solid solution of carbon in  $\alpha$  iron is termed  $\alpha$  ferrite, or simply ferrite. This phase has a BCC crystal structure, and at 0% C it corresponds to  $\alpha$  iron. The phase diagram indicates that carbon is only slightly soluble in ferrite since the maximum solid solubility of carbon in  $\alpha$  ferrite is 0.02 percent at 723°C. The solubility of carbon in  $\alpha$  ferrite decreases with decreasing temperature until it is about 0.008 percent at 0°C. The carbon atoms, because of their small size, are located in the interstitial spaces in the iron crystal lattice.

**AUSTENITE.** The solid solution of carbon in  $\gamma$  iron is designated *austenite*. It has a FCC crystal structure and a much greater solid solubility for carbon than  $\alpha$  ferrite. The solubility of carbon in austenite reaches a maximum of 2.08 percent at 1148°C and then decreases to 0.8 percent at 723°C (Fig. 1-2). As in the case of  $\alpha$  ferrite, the carbon atoms are dissolved interstitially, but to a much greater extent in the FCC lattice. This difference in the solid solubility of carbon in austenite and  $\alpha$  ferrite is the basis for the hardening of most steels.

**CEMENTITE.** The intermetallic Fe-C compound  $\text{Fe}_3\text{C}$  is called *cementite*. Iron carbide ( $\text{Fe}_3\text{C}$ ) has negligible solubility limits and contains 6.67% C and 93.3% Fe. Cementite, which is a hard and brittle compound, has an orthorhombic crystal structure with 12 iron atoms and four carbon atoms per unit cell (Fig. 1-3).

**$\delta$  FERRITE.** The solid solution of carbon in  $\delta$  iron is called  $\delta$  ferrite. It has a BCC crystal structure, but with a different lattice parameter than  $\alpha$  ferrite. The maximum solid solubility of carbon in  $\delta$  ferrite is 0.09 percent at 1495°C.

### Invariant Reactions in the Fe-Fe<sub>3</sub>C Phase Diagram

The Fe<sub>3</sub>C phase diagram of Fig. 1-2 has three invariant reactions, each of which occurs at constant temperature and involves three phases. These reactions are *peritectic*, *eutectic*, and *eutectoid*.

**PERITECTIC REACTION.** At the peritectic reaction point, liquid of 0.53% C combines with  $\delta$  ferrite of 0.09% C to produce  $\gamma$  austenite of 0.17% C. This reaction can be written as



Since this reaction occurs at such high temperatures, no  $\delta$  ferrite will normally be present in plain-carbon steels at room temperature.

**EUTECTIC REACTION.** At the eutectic reaction point, liquid of 4.3% C decomposes to produce  $\gamma$  austenite with 2.08% C and the intermetallic compound Fe<sub>3</sub>C (cementite), which contains 6.67% C. This reaction can be written as



Since plain-carbon steels do not contain more than about 1.2% C, the eutectic reaction will not be treated in the Fe-C alloy and steel chapters. This reaction will, however, be important in the study of cast irons, which contain above 2% C and which will be the subject of a later chapter.

**EUTECTOID REACTION.** At the eutectoid reaction point, solid austenite of 0.8% C decomposes into  $\alpha$  ferrite with 0.02% C and cementite with 6.67% C. This reaction can be written as



### Critical Temperatures

The temperature of 723°C is the critical temperature above which cementite becomes unstable when slowly heated under conditions approaching equilibrium. It is designated the  $A_1$  line<sup>1</sup> and is shown in Fig. 1-4. The symbol  $A$  is derived from the thermal *arrests* which are observed upon heating and cooling pure iron (Fig. 1-1). If high-purity plain-carbon steels with less than 0.8% C are heated above the  $A_3$  line,<sup>1</sup> all the ferrite in the steel is transformed into homogeneous austenite. Similarly, if high-purity plain-carbon steels with more than 0.8% C are heated above the  $A_{cm}$  line, all the cementite is transformed into homogeneous austenite.

<sup>1</sup> The designations  $A_{e_1}$  and  $A_{e_3}$  are sometimes used; the  $e$  subscript indicates *equilibrium* heating or cooling.

## Three invariant reactions in Fe-Fe<sub>3</sub>C phase diagram

- Peritectic reaction:



- Eutectic reaction:



- Eutectoid reaction:





# Critical temperatures

A = Thermal arrest

- $A_1$  line: eutectoid transformation
- $A_3$  line:  $\gamma$  transformation to  $\alpha$
- $A_{cm}$  line:  $\gamma$  transformation to  $Fe_3C$
- Cooling vs heating ( $A_r$  and  $A_c$ )

# Plain carbon steels

Fe-C steel alloys containing:

- from a trace to  $\sim 1.2\%C$
- minor amounts of other elements  
(Mn, Si, S, P, O, N)

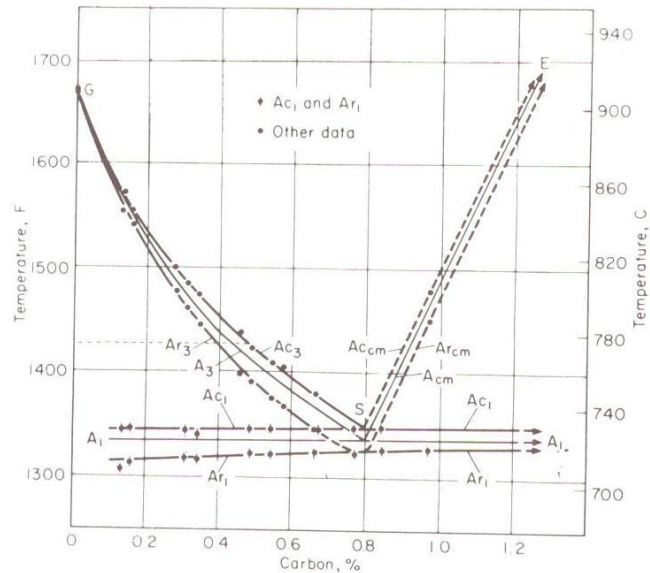


**FIGURE 1-4** Transformation temperatures in high-purity iron-carbon alloys. (After E. C. Bain and H. W. Paxton, "Alloying Elements in Steel," 2d ed., American Society for Metals, 1966, p. 20.)

When plain-carbon steels are heated or cooled through the transformation temperatures at faster than equilibrium rates, the transformation temperatures are displaced as indicated in Fig. 1-4. The thermal hysteresis (lag) which occurs upon rapid heating is indicated by the subscript *c* from the French word "chauffage" for heating. The thermal hysteresis which occurs on cooling is indicated by the subscript *r* from the French word "refroidissement" for cooling.

For example, the designation  $A_{r3}$  indicates the transformation temperature on rapid cooling a plain-carbon steel through the  $A_3$  transformation temperature. Thermal hysteresis is common in the industrial heat treatment of steel since the rapid heating and cooling of steels is frequently practiced.

### Eutectoid, Hypoeutectoid, and Hypereutectoid Plain-Carbon Steels

A plain-carbon steel containing 0.8% C is termed a *eutectoid* steel since the eutectoid transformation of austenite to cementite and ferrite occurs at this composition. If the carbon content of the steel is less than 0.8% C, it is designated a *hypoeutectoid* steel. Most steels produced commercially are hypoeutectoid steels.

Steels containing more than 0.8% C are called *hypereutectoid* steels. Hypereutectoid steels with up to about 1.2% C are produced commercially. When the carbon content of the steel goes beyond 1.2 percent, the steel becomes very brittle, and thus few steels are made with more than 1.2% C. In order to increase the strength of steels, other alloying elements are added which increase the strength as well as maintaining ductility and toughness.

### 1-3 SLOW COOLING OF PLAIN-CARBON STEELS

#### Eutectoid Plain-Carbon Steels

If a sample of a 0.8% plain-carbon steel is heated to about 750°C and held for a sufficient time, its structure will become homogeneous austenite. That is, the whole structure will become FCC austenite with the exception of some insoluble high-melting carbides or other impurity compounds. This process is called *austenitizing*.

If this eutectoid steel is slowly cooled under conditions approaching equilibrium, the structure will remain austenitic until just above the eutectoid temperature, as is indicated in Fig. 1-5 at point *a*. At the eutectoid temperature or slightly below it, if there is any undercooling, the entire structure will be

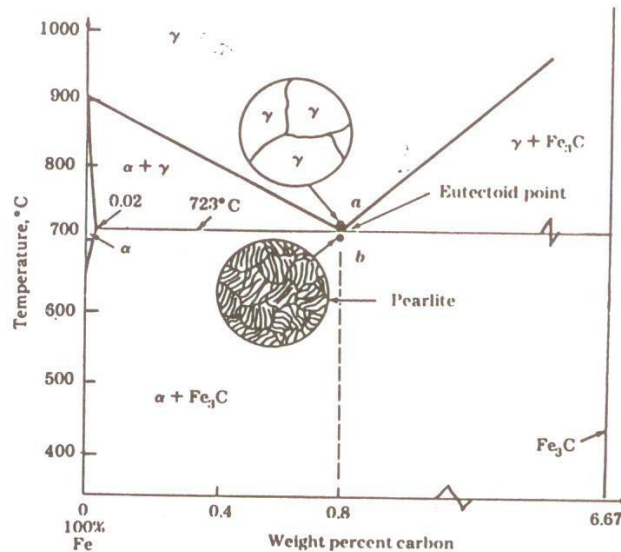


FIGURE 1-5 Transformation of an eutectoid steel (0.80% C) with slow cooling.



**FIGURE 1-6**

Microstructure of a slowly cooled eutectoid steel. The microstructure consists of lamellar eutectoid pearlite. The dark etched phase is cementite and the white phase is ferrite. (*United States Steel Co., as presented in Metals Handbook, 8th ed., vol. 8, American Society for Metals, 1973, p. 188.*)

transformed from austenite to a lamellar structure of alternate plates of  $\alpha$  ferrite and cementite ( $\text{Fe}_3\text{C}$ ). Just below the eutectoid temperature the lamellar structure will appear, as indicated at point *b* in Fig. 1-5.

Figure 1-6 shows a micrograph of an eutectoid steel that was slowly cooled in a furnace. Since this eutectoid structure as seen in the optical microscope resembles mother of pearl, it has been named *pearlite*. It should be noted that pearlite is not a single phase but a mixture of two phases,  $\alpha$  ferrite and cementite. The details of the nucleation and growth of this structure will be discussed in Sec. 1-5.

If the lever rule is applied to a slowly cooled 0.80% eutectoid steel at a temperature just under the eutectoid temperature of 723°C, the alloy should be composed of the following weight percentages of ferrite and cementite:

$$\text{Wt\% ferrite} = \frac{6.67 - 0.80\%}{6.67 - 0.02} \times 100\% = 88\%$$

$$\text{Wt\% cementite} = \frac{0.80 - 0.02}{6.67 - 0.02} \times 100\% = 12\%$$

Thus the pearlitic structure should consist of approximately 88% ferrite and 12% cementite at room temperature since the solubilities change very little from 723°C to room temperature. Also, since the densities of ferrite and cementite are approximately the same, the area ratio of the ferrite lamellae to those of the cementite should be about 7 : 1.

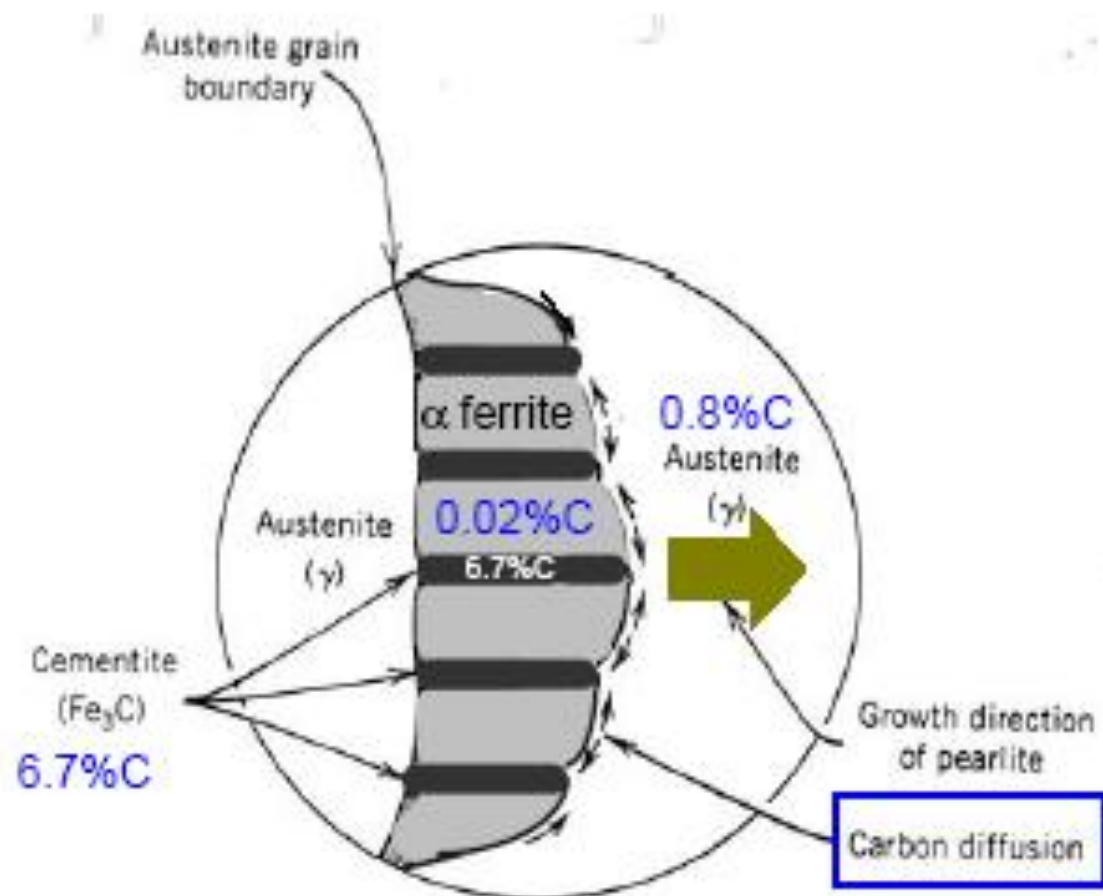
# Slow cooling of plain carbon steels

## Eutectoid alloy (Fe-0.77%C)

Austenite  Pearlite @727°C

- Microstructure: pearlite
  - lamellar eutectoid product alternates plates of  $\alpha$  and  $\text{Fe}_3\text{C}$
  - two phases grow simultaneously.
- Composition: lever rule

# Pearlite formation



# Slow cooling of plain carbon steels

## Hypoeutectoid alloy (Fe- $<0.77\%$ C)

$\gamma \xrightarrow{\text{slow cooling}}$  Proeutectoid  $\alpha$  +  $\gamma^l \xrightarrow{\text{slow cooling}}$  Proeutectoid  $\alpha$  + pearlite

- Microstructure: **Pearlite with ferrite along g.b's**
- Composition: lever rule
  - Ferrite grows by rejecting C to adjacent austenite
  - C diffuses down gradient in  $\gamma$  to obtain a homogeneous composition



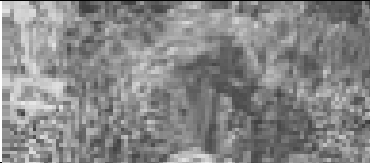



# Slow cooling of plain carbon steels

Hypereutectoid alloy ( $\text{Fe} > 0.77\% \text{C}$ )

$\gamma \longrightarrow \text{Proeutectoid Fe}_3\text{C} + \gamma^l \longrightarrow \text{Proeutectoid Fe}_3\text{C} + \text{pearlite}$

- Microstructure: **Pearlite with cementite along the g.b's**
- Composition: lever rule

# Summary

%C	Microstructure	Phase	Properties
0.8		100% P	Y.S. = 600 MPa
0		100% $\alpha$	Y.S. = 200 MPa
0.4		50% P 50% $\alpha$	Mixture of 2 phases: $\alpha$ = soft ductile ferrite with $<0.03\text{C}$
0.2		25% P 75% $\alpha$	P = $\alpha$ + $\text{Fe}_3\text{C}$ where $\text{Fe}_3\text{C}$ hard & brittle

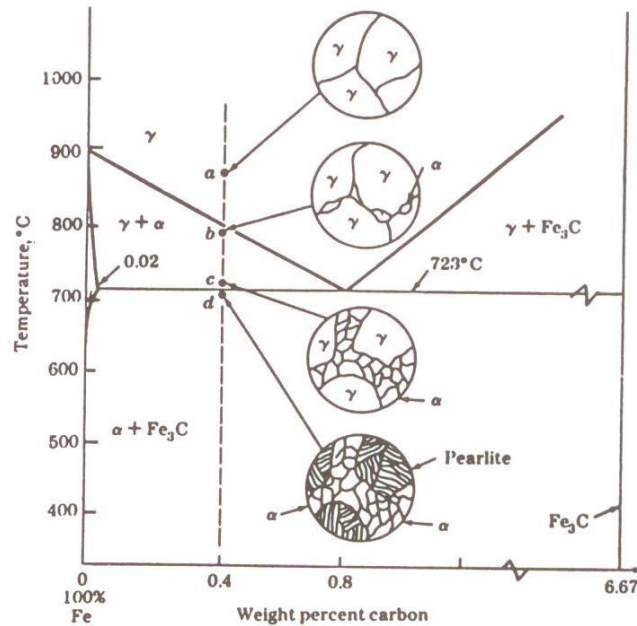


FIGURE 1-7 Transformation of a 0.4% carbon hypoeutectoid plain-carbon steel with slow cooling.

### Hypoeutectoid Plain-Carbon Steels

If a sample of a 0.4% plain-carbon steel (hypoeutectoid steel) is heated to about 900°C (point *a* in Fig. 1-7) for a sufficient time, its structure will become homogeneous austenite, as in the case of the eutectoid plain-carbon steel previously discussed. If this 0.4% C steel is then slowly cooled to the temperature shown at point *b* in Fig. 1-7 (about 775°C), *proeutectoid ferrite*<sup>1</sup> will begin to nucleate heterogeneously at the austenite grain boundaries. As the alloy is continuously cooled from the temperature at point *b* to that at *c* in Fig. 1-7, the proeutectoid ferrite will continue to grow into the austenite until about 50 percent of the sample is transformed. The excess carbon from the ferrite which is formed will be rejected at the austenite-ferrite interface into the remaining austenite, which becomes richer in carbon. While the alloy is cooled from the temperature at point *b* to that at *c*, the carbon content of the remaining

<sup>1</sup> The prefix "pro-" means "before," and thus the term *proeutectoid ferrite* is used to distinguish this constituent, which forms earlier, from eutectoid ferrite, which forms by the eutectoid reaction later in the cooling.

austenite will be increased from 0.4 to 0.8 percent. At 723°C, if conditions approaching equilibrium prevail, the remaining austenite will be converted to pearlite by the eutectoid reaction: austenite  $\rightarrow$  ferrite + cementite. The ferrite in the pearlite is called *eutectoid ferrite*, as contrasted to the proeutectoid ferrite which formed first. Both types of ferrite have the same composition under conditions approaching equilibrium.

Using the lever rule just slightly above 723°C at point *c* in Fig. 1-7, the weight percent proeutectoid ferrite and weight percent austenite can be calculated as

$$\text{Wt\% proeutectoid ferrite} = \frac{0.80 - 0.40}{0.80 - 0.02} \times 100\% = 50\%$$

$$\text{Wt\% austenite} = \frac{0.40 - 0.02}{0.80 - 0.02} \times 100\% = 50\%$$

Since all the remaining austenite will react to form pearlite at the eutectoid temperature of 723°C, the weight percent pearlite just slightly below 723°C at point *c* in Fig. 1-7 will be equal to the weight percent austenite just slightly above 723°C at point *b*. Thus there will be about 50% pearlite present in the 0.4% C steel at just under 723°C, if conditions approaching equilibrium exist.

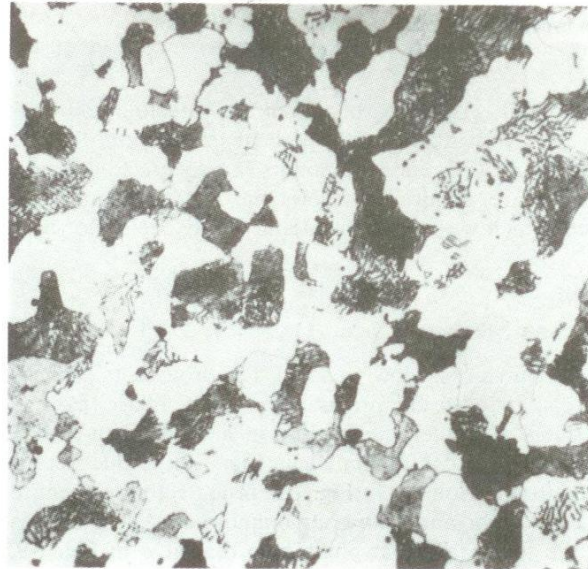


**FIGURE 1-8**

Microstructure of a 0.35% C hypoeutectoid steel. The white constituent in this microstructure is proeutectoid ferrite; the dark constituent is pearlite. (Etchant: 2% nital;  $\times 500$ .)

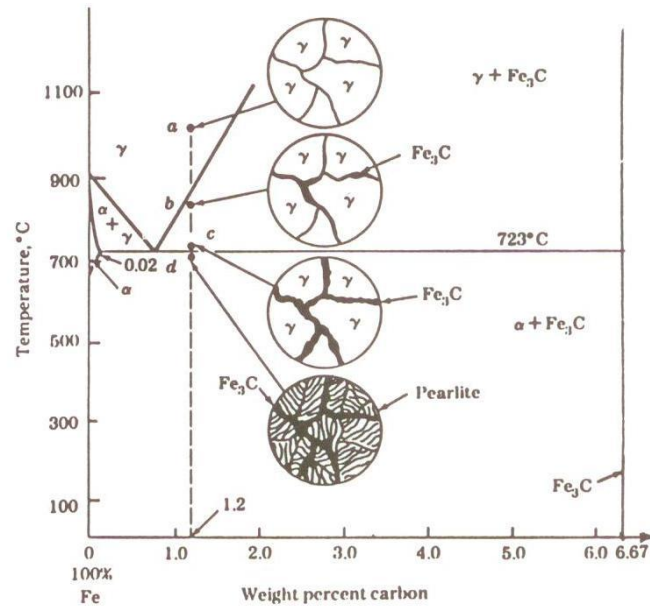


**FIGURE 1-9**  
Transformation of a 1.2% carbon hypereutectoid plain-carbon steel with slow cooling.

Since the decrease in solid solubility of the carbon from the eutectoid temperature to room temperature is very slight (i.e., 0.02 percent to near zero), there will be essentially no difference in the relative amounts of proeutectoid ferrite and pearlite at room temperature. Figure 1-8 shows the microstructure of a 0.35% C hypoeutectoid steel which was austenitized and slowly cooled to room temperature.

### Hypereutectoid Plain-Carbon Steels

If a hypereutectoid plain-carbon steel is slowly cooled, the proeutectoid phase in this case is *cementite*, as contrasted to the proeutectoid ferrite phase that was formed in hypoeutectoid steels. Consider the cooling of a 1.2% plain-carbon steel which has been austenitized at 950°C (point *a* in Fig. 1-9). If this steel is slowly cooled to the temperature at point *b* in Fig. 1-9, proeutectoid cementite will begin to nucleate and grow at the austenite grain boundaries. As the alloy is continuously cooled from the temperature at point *b* to that at *c* in Fig. 1-9, proeutectoid cementite will continue to form and deplete the carbon from the remaining austenite at the austenite-cementite interfaces. If conditions approaching equilibrium are present during cooling from the temperature at point *b* to that at *c*, the overall carbon content of the austenite will be decreased from



1.2 to 0.8 percent. At 723°C, the remaining austenite will be transformed to pearlite by the eutectoid reaction. The cementite in the pearlite is referred to as “eutectoid cementite” to differentiate it from the proeutectoid cementite.

Using the lever rule just slightly above 723°C at point *c* in Fig. 1-9, the weight percent proeutectoid cementite and austenite can be calculated as

$$\text{Wt\% proeutectoid cementite} = \frac{1.2 - 0.80}{6.67 - 0.80} \times 100\% = 6.8\%$$

$$\text{Wt\% austenite} = \frac{6.67 - 1.2}{6.67 - 0.80} \times 100\% = 93.2\%$$

Since all the remaining austenite will be transformed into pearlite at the eutectoid temperature of 723°C, the weight percent pearlite just below 723°C at point *d* will be equal to the weight percent austenite just slightly above 723°C at point *c*. Thus there will be about 93.2% pearlite present in the 1.2% C steel at just under 723°C, if conditions approaching equilibrium exist. Since the decrease in solid solubility of carbon in ferrite from 723°C to room temperature is very slight, the same relative amounts of cementite and pearlite will be present at room temperature.

It is interesting to note that at 0.4% C in the hypoeutectoid steel, there is 50% proeutectoid ferrite, while in the 1.2% hypereutectoid steel, there is only

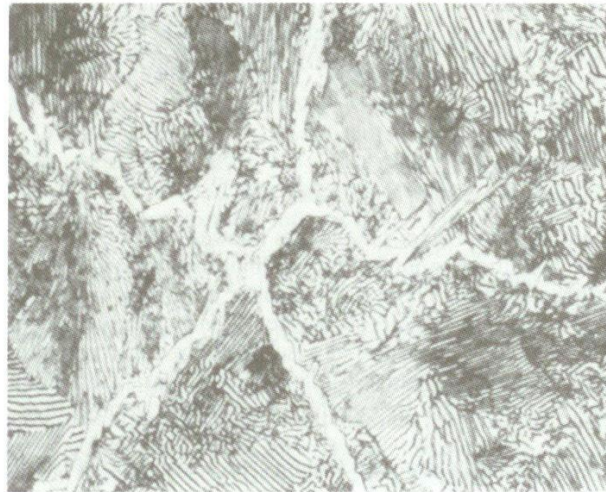
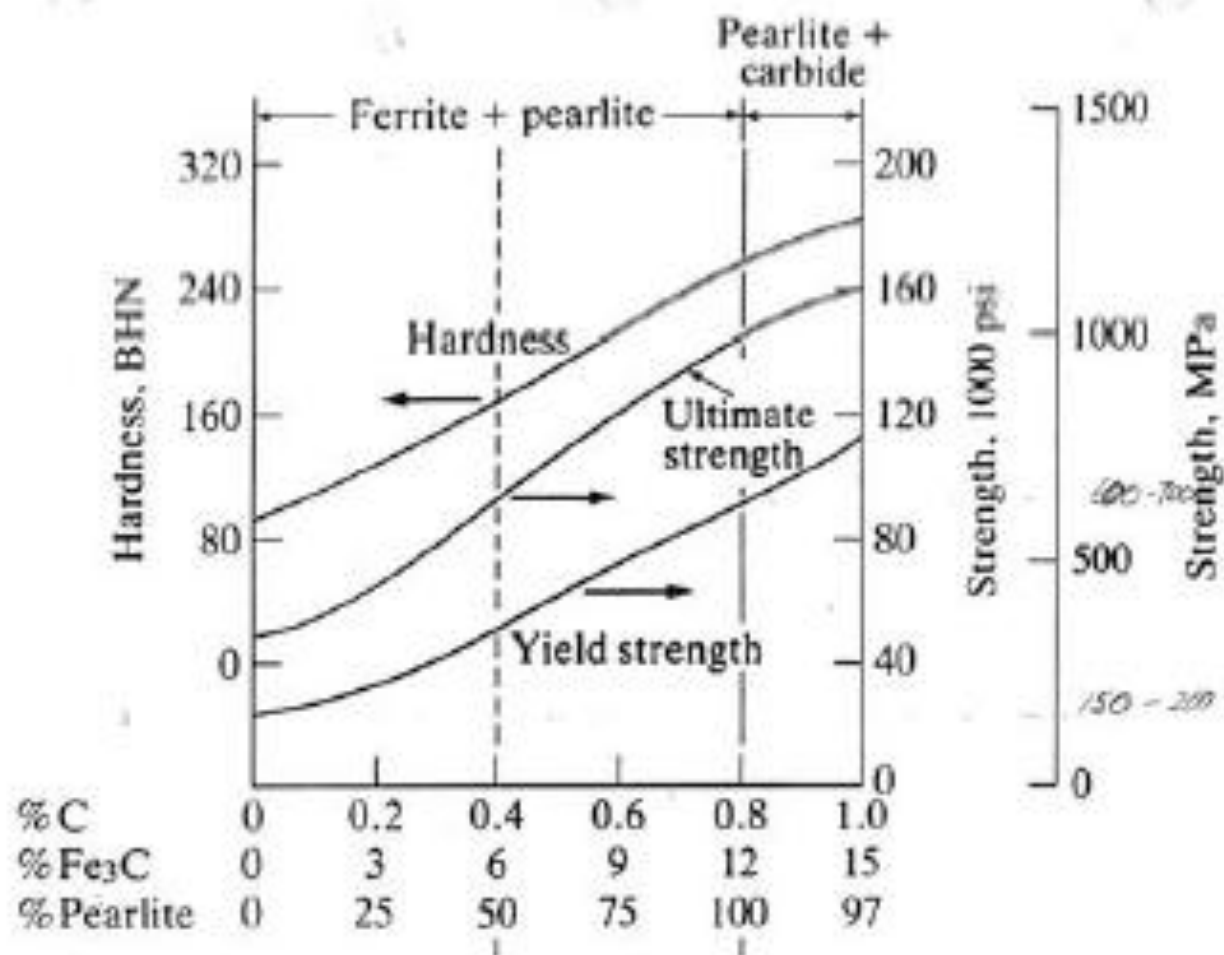


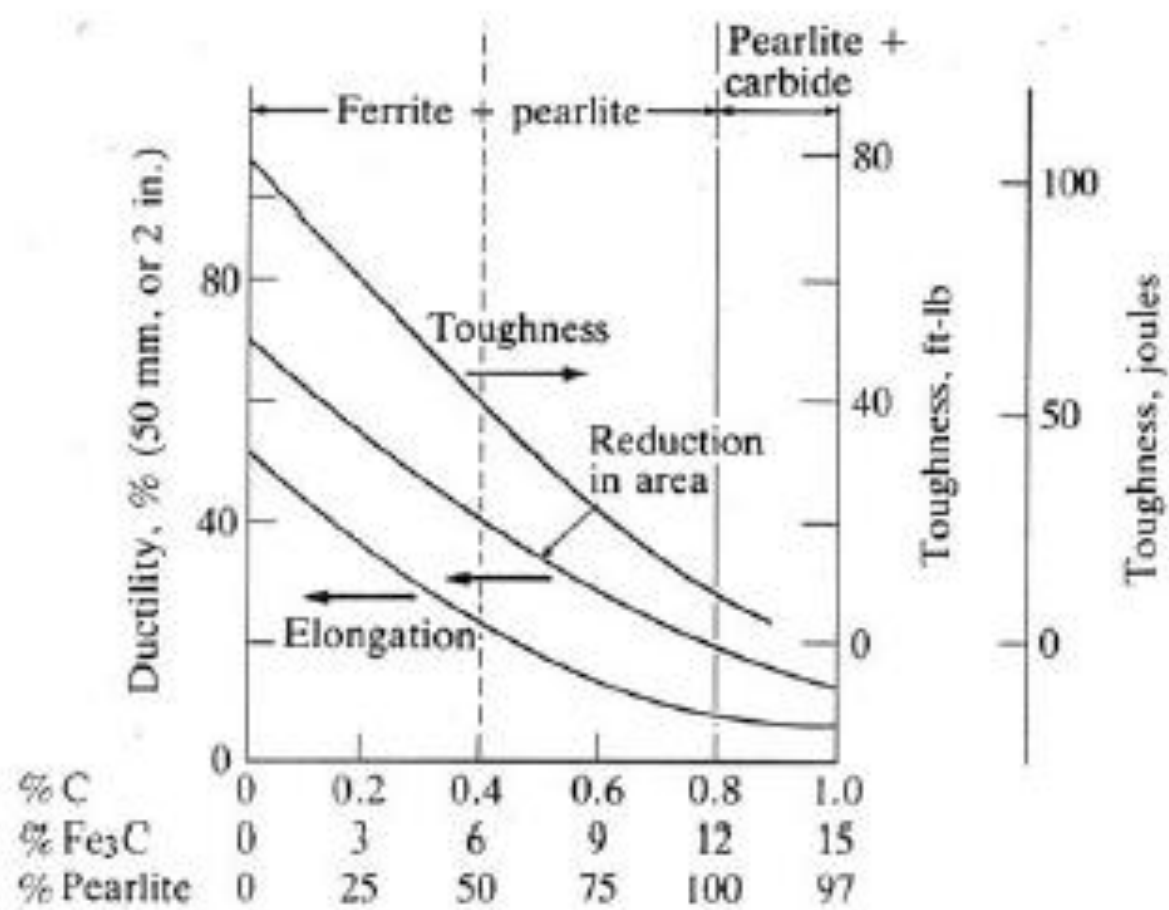
**FIGURE 1-10**

Microstructure of a 1.2% carbon hypereutectoid steel. In this structure the cementite appears as the white platelike constituent which has formed at the former austenite grain boundaries. The remaining structure consists of lamellar pearlite. (Etchant: picral;  $\times 1000$ .) (Courtesy of United States Steel Research Laboratory.)

# Hardness & microstructure



# Toughness & microstructure





# Applications

## 100% $\alpha$

- sheet steel
- car panels
- roofing
- cans

## 100% **P**

- rails
- (cold worked to give high strength)
- cable
- prestressed tendons for concrete

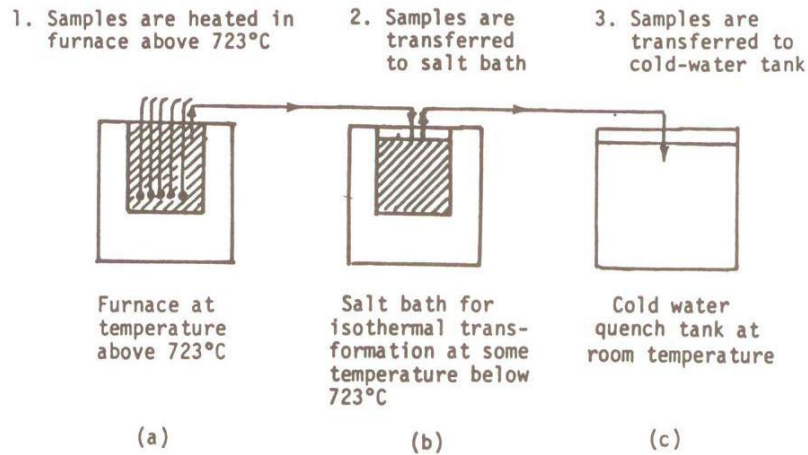


FIGURE 1-11

Experimental arrangement for determining the microscopic changes that occur during the isothermal transformation of austenite in an eutectoid plain-carbon steel.

6.8% proeutectoid cementite. This difference is quite apparent in comparing the microstructure of the 0.4% C steel of Fig. 1-8 with that of the 1.2% C steel in Fig. 1-10. The reason for this difference in proeutectoid constituent is that in the case of the 0.4% C steel, the  $(\gamma + \alpha)$  phase field extends *only from* 0.025 to 0.8% C. However, in the case of the 1.2% C steel, the  $(\gamma + \text{Fe}_3\text{C})$  phase field extends from 0.8 to 6.67% C.

#### 1-4 ISOTHERMAL TRANSFORMATION OF AN EUTECTOID PLAIN-CARBON STEEL

In the previous section, an eutectoid steel sample was allowed to cool slowly to room temperature under conditions approaching equilibrium, and it thereby produced a coarse pearlitic structure. Let us now consider what happens to the microstructure of an austenitized eutectoid steel when it is rapidly cooled to temperatures below the eutectoid temperature and isothermally transformed. In this way the austenitic decomposition can be followed as the transformation progresses by examining the microstructures of the samples after various intervals.

In such isothermal transformation experiments of an eutectoid steel, which were first made by Davenport and Bain,<sup>1</sup> small thin-steel samples about the size of a dime are first austenitized in a furnace at a temperature above the

<sup>1</sup> E. S. Davenport and E. C. Bain. *Trans. AIME* 90(1930):117.

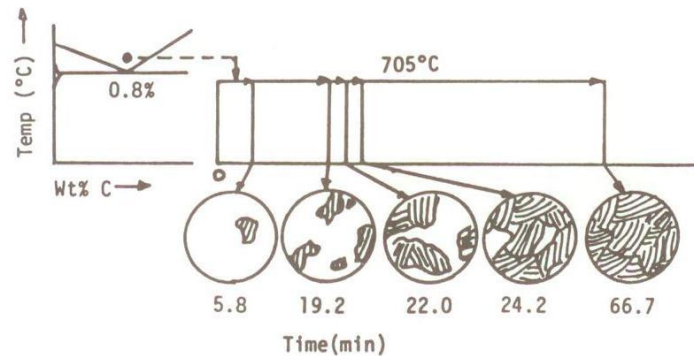


FIGURE 1-12

Experiment for following the microstructural changes which occur during the isothermal transformation of an eutectoid plain-carbon steel at 705°C. After austenitizing, samples are quenched in salt bath at 705°C, held for times indicated, and then quenched in water at room temperature.

eutectoid temperature (Fig. 1-11a). The samples are then rapidly quenched (cooled) in a salt bath at the desired temperature below the eutectoid temperature (Fig. 1-11b). After various time intervals, the samples are removed from the salt bath, one at a time, and quenched into water at room temperature (Fig. 1-11c). The microstructure after each transformation time can then be examined at room temperature.

Consider the isothermal transformation of a 0.80% eutectoid plain-carbon steel, as is illustrated in Fig. 1-12. The steel samples are first austenitized at 760°C, which results in a polycrystalline austenitic structure as shown in Fig. 1-13a. Five small (dime-shaped) samples are then quenched into a salt bath at 705°C. After 5.8 min at 705°C, pearlite begins to nucleate and grow at the austenitic grain boundaries (Fig. 1-13b). After 19.2 min about 25 percent of the austenite is transformed into pearlite (Fig. 1-13c). The transformation now accelerates and after 22 min, 50 percent of the austenite transforms into pearlite (Fig. 1-13d). In just over 2 min more, making a total of 24.2 min, 75 percent of the austenite is transformed to 75% pearlite (Fig. 1-13e). The reaction now slows down due to the impingement of the pearlite nodules, and after 66.7 min it is complete (Fig. 1-13f).

By repeating the same procedure for progressively lower temperatures, an isothermal transformation diagram such as is shown schematically in Fig. 1-14 can be constructed. Since this diagram involves time, temperature, and transformation, it is sometimes called a TTT diagram. However, this type of diagram is best referred to as an IT (isothermal transformation) diagram to distinguish it from a CCT or “continuous-cooling transformation” diagram.

When eutectoid plain-carbon steels are isothermally transformed at temperatures in the upper section of the IT diagram, from about 550 to 723°C, austenite transforms to *pearlite*. If the eutectoid steel is quenched from the

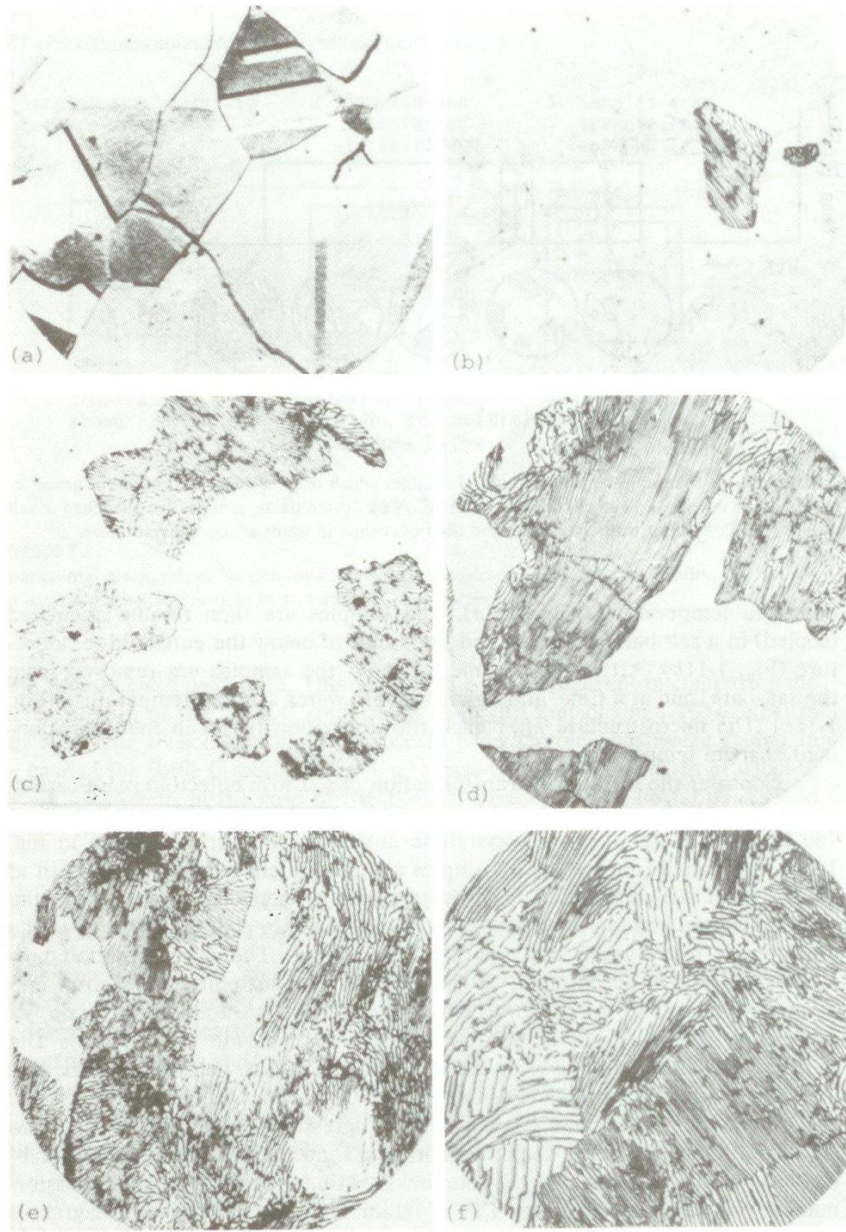


**FIGURE 1-13**

Microstructures showing the changes in the isothermal transformation of austenite to pearlite in an eutectoid plain-carbon steel at 705°C. (a) Austenite, (b) after 5.8 min, (c) after 19.2 min, (d) after 22 min, (e) after 24.2 min, (f) after 66.7 min. (Etchant: picral;  $\times 1000$ .) (After J. Vilella, E. C. Bain and H. W. Paxton, in "Alloying Elements in Steel," 2d ed., American Society for Metals, 1966, pp. 21-26.)



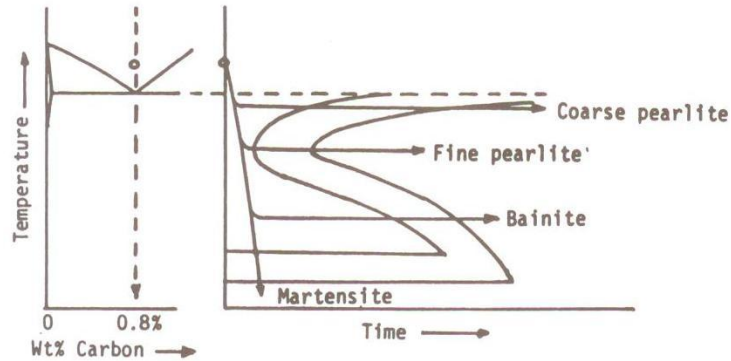


FIGURE 1-14

Isothermal transformation diagram for an eutectoid plain-carbon steel showing its relationship to the Fe-Fe<sub>3</sub>C phase diagram.

austenitizing temperature to room temperature, a new metastable phase called *martensite* is formed. Martensite is essentially a supersaturated solid solution of carbon in  $\alpha$  ferrite. If the eutectoid steel is quenched to some temperature between about 250 and 550°C and is isothermally transformed, an intermediate structure between pearlite and martensite is formed. This structure is called *bainite* after E. C. Bain, and shows characteristics intermediate between pearlite and martensite. A summary of pearlitic, martensitic, and bainitic microstructures associated with the isothermal transformation diagram are shown in Fig. 1-15.

## 1-5 TRANSFORMATION OF AUSTENITE TO PEARLITE

### Mechanism and Morphology

If a homogeneous sample of an eutectoid steel is quenched from the austenite region to some particular temperature between 723 and 550°C, the nucleation and growth of pearlite will occur as indicated in the isothermal transformation diagram of Fig. 1-16. The microstructures of the progressive stages of the formation of coarse pearlite by isothermal transformation at 705°C have already been shown in Fig. 1-13. In this section some of the details of the austenite-to-pearlite transformation will be discussed.

**NUCLEATION AND GROWTH OF PEARLITE LAMELLAE.** If the austenite is homogeneous, nucleation of the pearlite will occur first at the grain boundaries, since they are energetically favorable nucleation sites and have faster paths for diffusion than areas within the grains. Since the nucleation of pearlite occurs so

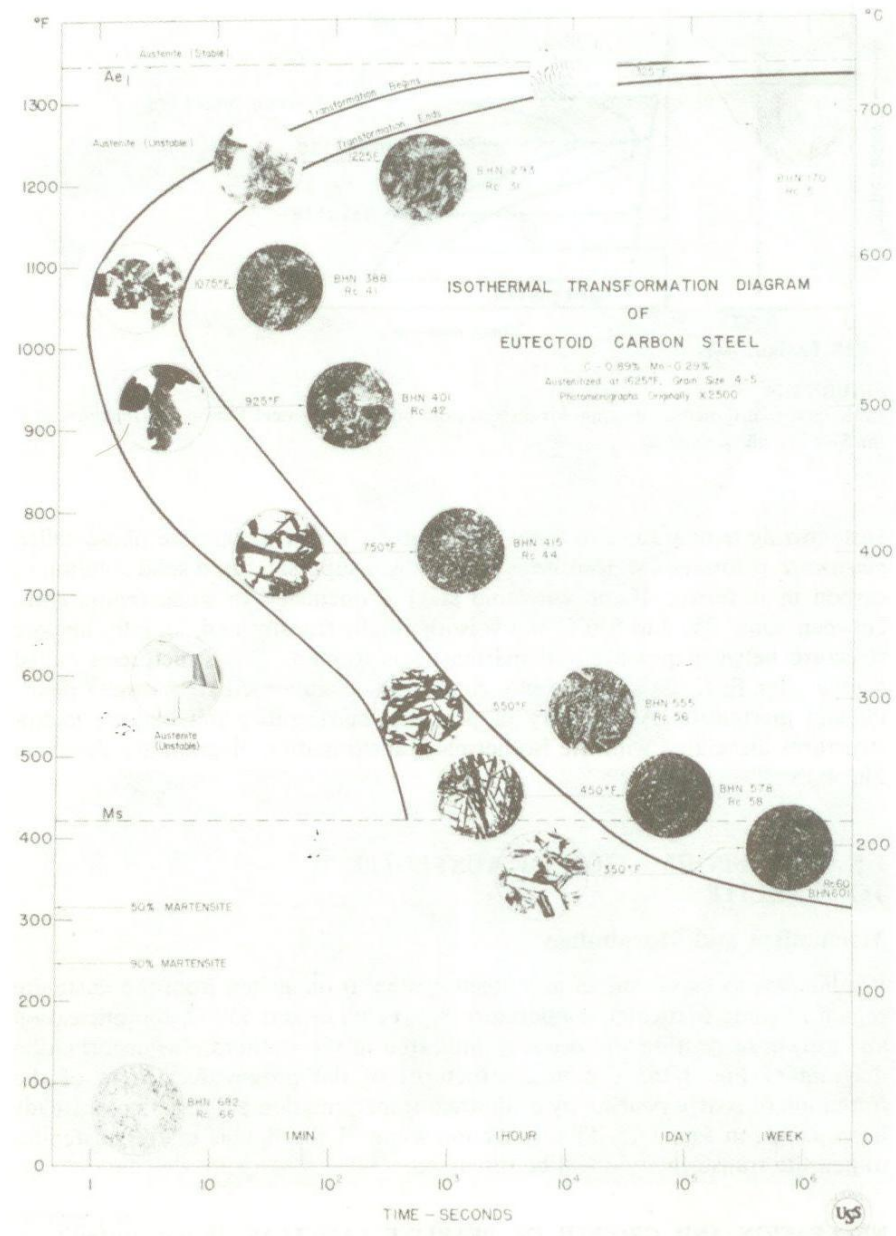


**FIGURE 1-15**

Isothermal transformation diagram of an eutectoid steel. (Courtesy of United States Steel Co., Research Laboratory.)

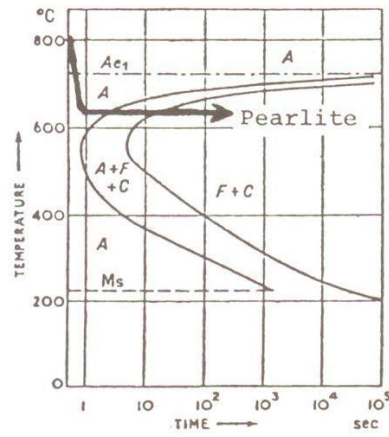


**FIGURE 1-16**  
Isothermal transformation diagram for an eutectoid steel indicating the cooling path for the formation of pearlite.

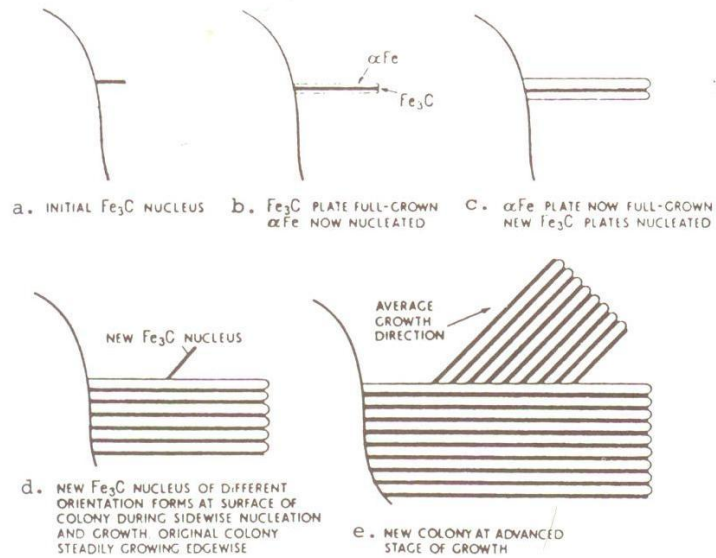


**FIGURE 1-17**  
The nucleation and growth of pearlite. [After R. F. Mehl, *Trans. ASM* 29 (1941):813, as presented in "Progress in Metal Physics," vol. 6, 1956, p. 92, Pergamon. Reprinted with permission.]

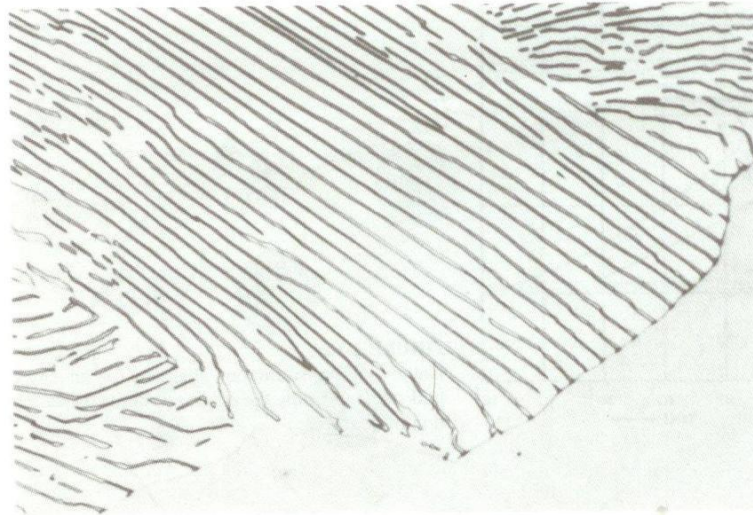


**FIGURE 1-18**

Eutectoid steel that has partially transformed to pearlite at 700°C. (After J. R. Vilella, United States Steel Co., Research Laboratory.)

rapidly in a plain-carbon steel, it is extremely difficult to determine the nucleation mechanism. However, by slowing down the nucleation process by the addition of 12% Mn to an eutectoid steel, it has been shown by thin-foil microscopy that either ferrite or cementite can nucleate pearlitic nodules.<sup>1</sup>

Let us assume in the nucleation of pearlite that a cementite lamella is formed first (Fig. 1-17*a*). The austenite in the region adjacent to the cementite will be depleted of carbon and, as a consequence, when the carbon content of the austenite decreases to a low enough level, adjacent layers of ferrite will form (Fig. 1-17*b*). The ferrite plate will grow straight ahead into the austenite as well as sideways until a sufficient amount of carbon is rejected so that new carbon lamellae can be produced (Fig. 1-17*c*). Eventually, a new side nucleus of cementite can form and start a new colony advancing in another direction (Fig. 1-17*d* and *e*). The structure of an eutectoid steel that has been partially transformed into pearlite at 700°C is shown in Fig. 1-18.

The growth of pearlite from austenite during isothermal transformation is always nodular, as is shown in the hot-stage micrograph in Fig. 1-19. The pearlitic nodules grow from the nuclei along the austenitic boundaries and continue to grow radially until they impinge on one another. Within each

<sup>1</sup> R. J. Dippenaar and R. W. K. Honeycombe, *Proc. Roy. Soc. London* A333(1973):455.



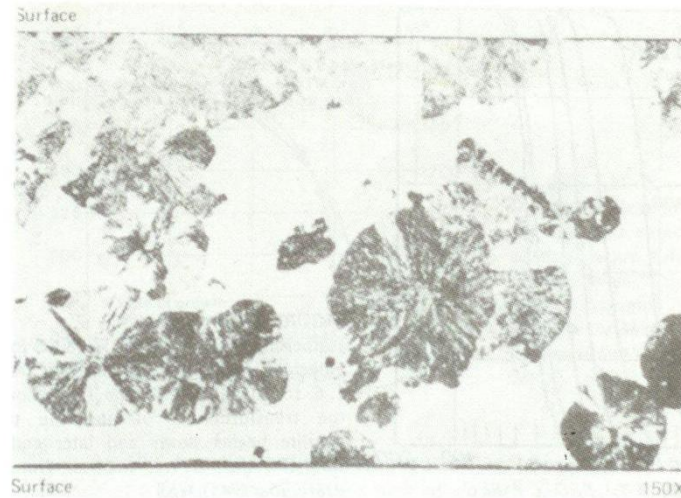


**FIGURE 1-19**

Cross-section view of the microstructure of pearlite nodules in partially transformed hot-stage specimen showing nodules forming at both specimen surface and interior. [After B. L. Bramfitt and A. R. Marder, *Metall. Trans.* 4(1973):2291.]

pearlitic nodule there are colonies of alternating ferrite and cementite lamellae, all with the same orientation.

A plot of the percent pearlite transformed versus time produces a sigmoidal curve (Fig. 1-20a). In the first stage, the transformation rate of austenite to pearlite is slow since only a few pearlitic nodules are nucleated and grow. This stage may be considered an incubation period. In the second stage, the transformation rate is greatly accelerated since many new nuclei are formed and grow, while the growth of the existing nodules continues. The growth rate of the

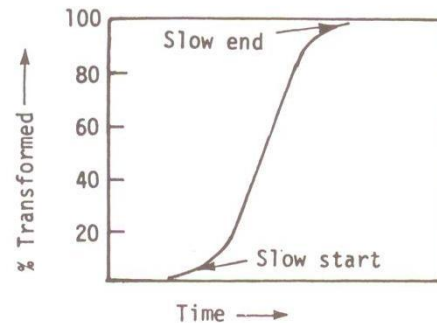


**FIGURE 1-20a**

Idealized isothermal reaction curve.

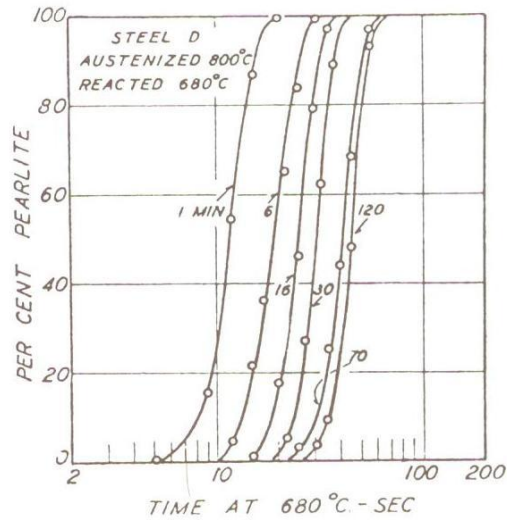


**FIGURE 1-20b**  
Isothermal reaction curves at 680°C for eutectoid steel austenitized at 800°C for 1, 6, 16, 30, 70, and 120 min. (Note how the transformation of austenite to pearlite begins slowly and later ends slowly.) [After G. A. Roberts, *Trans. AIME* 154(1943):318.]

pearlite at any instant is proportional to the area of austenite-pearlite interface at that time. Finally, a third stage is reached when the transformation rate decreases since the nucleation rate is decreased and continued growth of the existing pearlitic nodules is hampered by their impinging on each other (Fig. 1-20b).

### Effects of Temperature

The decomposition of austenite to pearlite involves two important variables, both of which are ultimately temperature-dependent. These are the nucleation rate  $N$  of the pearlite, and the growth rate  $G$ . The nucleation rate, which is the number of nuclei formed in a unit volume in a unit time, increases as the temperature of the transformation is lowered. Thus, as the  $\Delta T$  of undercooling below the  $A_{e1}$  is increased, more nuclei are available to form pearlite. The growth rate is diffusion-dependent, and hence, as the temperature of the transformation decreases, the growth rate decreases also.

The transformation rate of austenite to pearlite at a specific temperature will therefore depend on the rate of nucleation of the pearlite,  $N$ , and the growth rate  $G$  of the pearlitic nodules. At relatively high temperatures, i.e., slightly below 723°C, the  $A_{e1}$  temperature, the nucleation rate will be relatively low due to the small  $\Delta T$  and the growth rate high due to a high diffusion rate (Fig. 1-21). Thus the ratio  $N/G$  will be small. At this temperature, the nuclei will grow rapidly into large pearlitic nodules which can cross grain boundaries and consume large numbers of austenitic grains before impinging on one another.

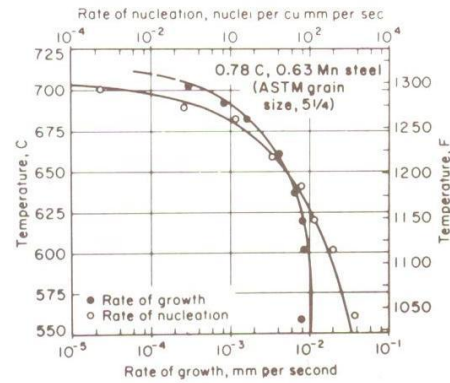


**FIGURE 1-21**

Rates of nucleation and growth of pearlite colonies in an eutectoid steel as a function of temperature. (After R. F. Mehl and W. C. Hagel from "Progress in Metal Physics," vol. 6, Pergamon, 1956, p. 102, as presented in the Metals Handbook, 8th ed., vol. 8, American Society for Metals, 1973, p. 189.)

As the transformation temperature is lowered, the nucleation rate increases at a faster rate than the rate of growth, as is also indicated in Fig. 1-21. Thus the ratio  $N/G$  will become larger. As a result, at the early stages of the transformation, the austenitic grain boundaries will be outlined by pearlitic nodules that form by nucleation and growth. This is clearly shown in the eutectoid steel of Fig. 1-22, which is in the early stages of transformation at 550°C.

The interlamellar spacing of the pearlite decreases as the transformation temperature decreases since, with a high nucleation rate, the carbon atoms do not have to migrate as far in forming the ferrite-cementite lamellae. The increased free energy from the transformation due to the large degree of

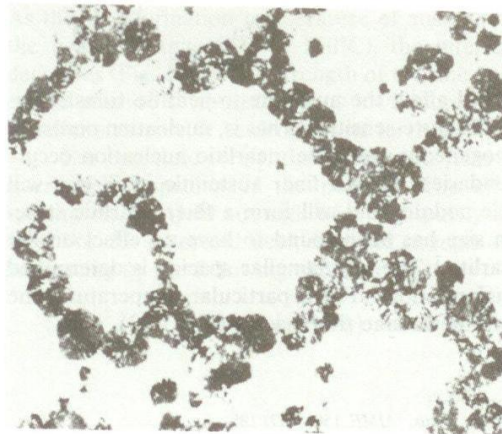


**FIGURE 1-22**

Eutectoid steel partially transformed to pearlite at 550°C. (Note how the pearlite outlines the austenite grain boundaries.) (After H. Aaronson, from P. G. Shewmon, "Transformations in Metals" McGraw-Hill, 1969, p. 228.)

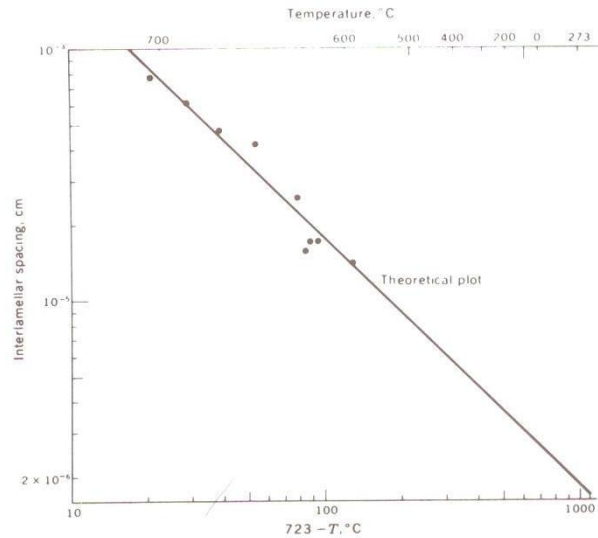


**FIGURE 1-23**

Relationship between interlamellar spacing and degree of undercooling in an eutectoid steel. [After G. E. Pellisier, M. F. Hawkes, W. A. Johnson, and R. F. Mehl, *Trans. ASM* 29(1942):1049, as presented in P. G. Shewmon, "Transformations in Metals," McGraw-Hill, 1969, p. 232.]

undercooling ( $\Delta T$ ) supplies sufficient energy to provide the large interfacial energy of the fine ferrite-cementite lamellae formed at the lower temperatures. Figure 1-23 shows how the interlamellar spacing of the pearlite in an eutectoid steel decreases with decreasing temperature.

### Effects of Grain Size

The grain size of the austenite will affect the austenite-to-pearlite transformation since the nucleation rate is structure-sensitive. That is, nucleation occurs in regions of high energy. In homogeneous austenite, pearlitic nucleation occurs almost exclusively at grain boundaries. Thus a finer austenitic grain size will provide more nuclei for pearlitic nodules and will form a finer pearlitic structure. The prior austenitic grain size has been found to have no effect on the interlamellar spacing of the pearlite.<sup>1</sup> The interlamellar spacing is determined by the temperature of the transformation.<sup>2</sup> For a particular temperature, the nucleation and diffusion rates will determine this spacing (Fig. 1-23).

<sup>1</sup> F. C. Hull, R. A. Colten, and R. F. Mehl, *Trans. AIME* 150(1942):185.

<sup>2</sup> G. E. Pellisier, M. F. Hawkes, W. A. Johnson, and R. F. Mehl, *Trans. ASM* 29(1942):1049.



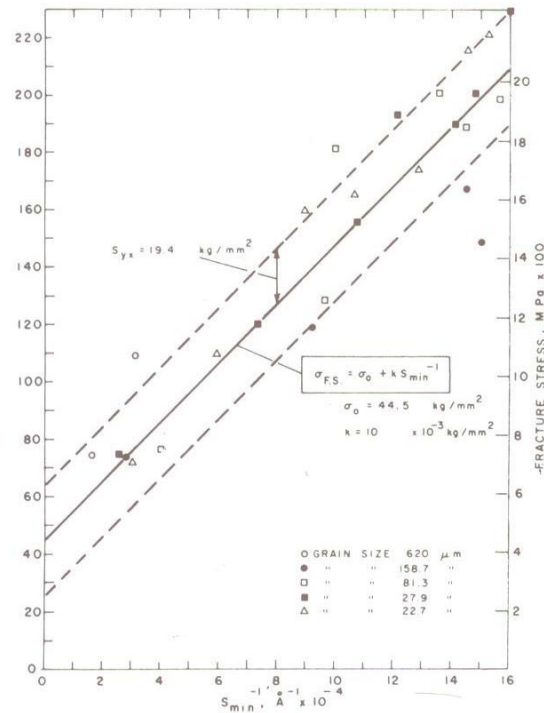


**FIGURE 1-24**  
 Effect of minimum interlamellar spacing of pearlite in an eutectoid steel on yield strength. [After A. R. Marder and B. L. Bramfitt, *Metall. Trans.* 7A(1976):365.]

### The Strength of Pearlite<sup>1</sup>

In general, the pearlitic structure is softer than the martensitic or bainitic types. As the transformation temperature of austenite to pearlite is decreased within the pearlitic range (723 to 550°C), the interlamellar spacing of the pearlite decreases (Fig. 1-23). The strength of the fine pearlite is greater than that of the coarse pearlite since dislocations have more difficulty passing through the fine lamellar structure of cementite and ferrite.

For eutectoid steels, the increase in yield strength varies inversely as the interlamellar spacing of the pearlite. The effect of minimum interlamellar spacing on the yield strength of a high-purity eutectoid steel is shown in Fig. 1-24. For this eutectoid steel, the yield strength can be related to the interlamellar spacing by the following expression:

$$\sigma_y(\text{MPa}) = 139 + 46.4S^{-1}$$

<sup>1</sup> A. R. Marder and B. L. Bramfitt, *Metall. Trans.* 7A(1976):365.

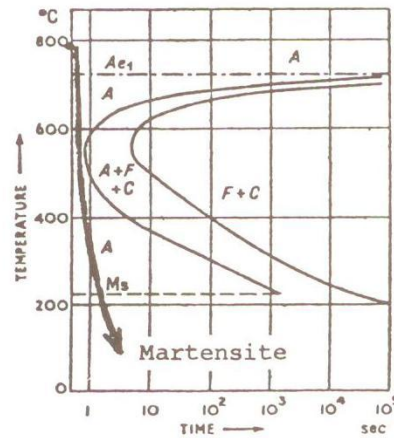


**FIGURE 1-25**  
Isothermal transformation diagram for an eutectoid steel indicating the cooling path for the formation of martensite.

## 1-6 TRANSFORMATION OF AUSTENITE TO MARTENSITE

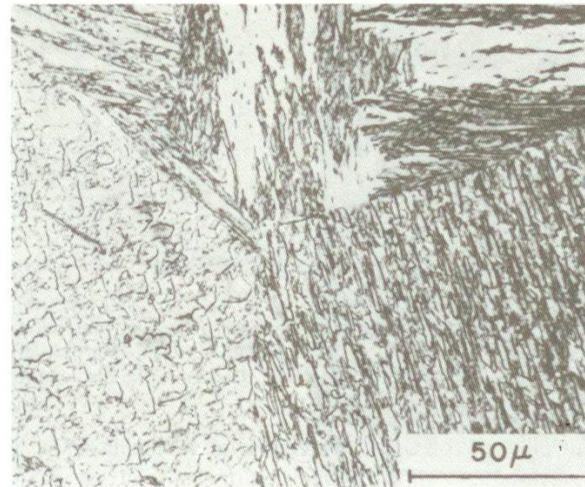
If a plain-carbon eutectoid steel (Fe-0.8% C) is cooled rapidly from the austenitic region so that it misses the nose of the IT curve (Fig. 1-25), a new phase called *martensite* is formed at temperatures below about 220°C. Martensite in steels is a metastable structure consisting of a supersaturated solid solution of carbon in  $\alpha$  ferrite. The study of the martensitic transformation in steels is of great engineering importance because of the ability of martensite to harden and strengthen many steels.

This section on martensite will begin with a description of its characteristics, which will be followed by an examination of its morphological changes with variation in carbon content. Then, a brief discussion of its mechanisms and kinetics of formation will be given. Finally, some information on the strength of martensite will be presented.

### Characteristics of the Martensitic Transformation in Plain-Carbon Steels

1. An important characteristic of the martensitic transformation in plain-carbon steels is that various microscopically observable structures are produced by it and that *the type of martensitic structure obtained depends on the carbon content of the steel.*<sup>1</sup> If the carbon content of the steel is low (i.e., about 0.2 wt%), then well-defined laths of martensite are observed in the optical microscope (Fig. 1-26a). As the carbon content is increased (i.e., to about

<sup>1</sup>A. R. Marder and G. Krauss, *Trans. ASM* 60(1967):651.



(a)

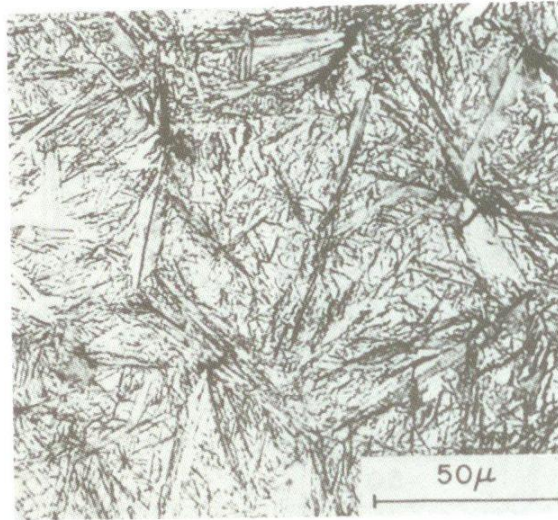


(b)

**FIGURE 1-26**

Effect of carbon content on the structure of martensite in plain-carbon steels: (a) lath type; (b) mixed lath and plate types, arrow points to a plate; (c) plate type. (Etchant: sodium bisulfite; optical micrographs.) [After A. R. Marder and G. Krauss, *Trans. ASM* 60(1967):651.]





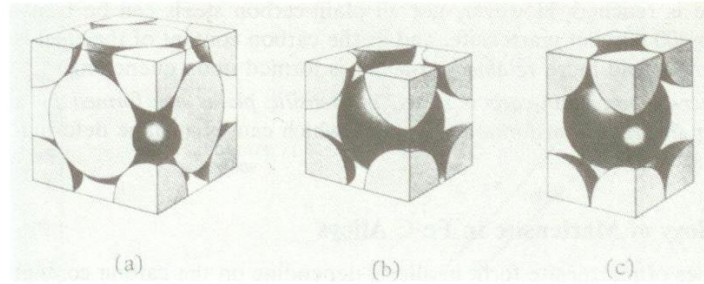
(c)

FIGURE 1-26 (Continued)

0.6 wt%), plates of martensite begin to form, as is pointed out in Fig. 1-26*b*. If the carbon content is increased still more to about 1.2 wt%, the martensite appears as an array of well-defined plates (Fig. 1-26*c*). This sequence of optical micrographs shows how the type of martensite formed depends on the carbon content of the steel.

2. Another important characteristic of the martensitic transformation is that it is *diffusionless*. That is, the reaction takes place so rapidly that atoms do not have time to intermix. There appears to be no thermal activation energy barrier to prevent its formation.
3. There appears to be *no compositional change* in the parent phase after the martensitic reaction, and each atom tends to preserve its own original neighbors. The relative positions of the carbon atoms with respect to the iron atoms are the same in the martensite as they were in the austenite.
4. *The crystal structure produced by the martensitic transformation in plain-carbon steels changes from BCC to body-centered tetragonal (BCT) as the carbon content of the steel is increased.* For low carbon contents less than about 0.2 wt%, the austenite transforms to a BCC  $\alpha$  ferrite crystal structure. When the carbon content of the steel is increased, the BCC structure is distorted into a BCT crystal structure. The BCT structure is produced primarily because of the greater solid solubility difference of carbon in FCC austenite and BCC ferrite iron. Figures 1-27*a* and *b* show that the interstitial spaces for the carbon atoms are much larger in the FCC unit cell than in the BCC unit cell.





**FIGURE 1-27**

Interstitial positions of carbon atoms in FCC, BCC, and BCT iron-crystal structure unit cells. (After E. R. Parker and V. F. Zackay, "Strong and Ductile Steels," *Scientific American*, November 1968, p. 36. Used by permission.)

This change in interstitial spacing leads to the distortion of the BCC unit cell along the  $c$  axis to accommodate the excess carbon atoms (Fig. 1-27c).

5. The martensitic transformation in steel starts at a definite temperature called the  $M_s$  (Fig. 1-28). When austenitized Fe-C alloys are quenched, martensite starts to form as the temperature of the alloys reaches the  $M_s$ . As the temperature continues to be lowered during cooling, more and more of the austenite is transformed into martensite until the  $M_f$  (martensitic finish)

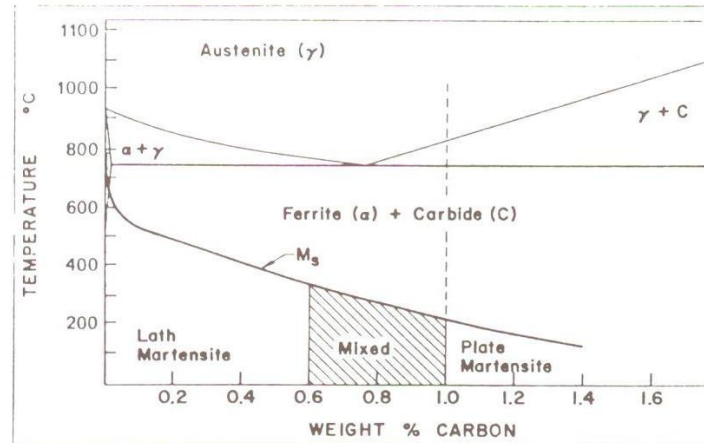


**FIGURE 1-28**

Effect of carbon content on the martensite transformation start temperature,  $M_s$ , for iron-carbon alloys. (After A. R. Marder and G. Krauss, as presented in "Hardenability Concepts with Applications to Steel," *AIME* 1978, p. 238.)

temperature is reached. However, not all plain-carbon steels can be transformed into 100 percent martensite, and as the carbon content of the steel is increased, more and more *retained austenite* is formed upon quenching.

6. In the higher-carbon plain-carbon steels, martensitic plates are formed by a displacive or shearlike transformation process which causes a shape deformation on a flat surface.

### The Morphology of Martensite in Fe-C Alloys

Two major types of martensite form in alloys, depending on the carbon content of the plain-carbon steels. These are Type I, or *lath* martensite, and Type II, or *plate* martensite. The lath martensite is predominant in Fe-C alloys with up to about 0.6% C (Fig. 1-28). Above about 1.0% C, the plate-type martensite predominates, while between 0.6 and 1.0% C, a transition from lath to plate types takes place. In this region, therefore, mixed structures of both types appear.

**TYPE I—LATH MARTENSITE.** In low-carbon Fe-C alloys, the martensite consists of domains which have groups of laths separated by low-angle or high-angle grain boundaries (Fig. 1-26*a*). The structure within the martensitic laths is highly distorted, consisting of regions with high densities of dislocation tangles (Fig. 1-29). The structure of low-carbon lath martensites consists of a regular



**FIGURE 1-29**

Structure of lath martensite in an Fe-0.2% C alloy. (Note the parallel alignment of the laths.) [After A. R. Marder and G. Krauss, *Trans. ASM* 60(1967):651.]

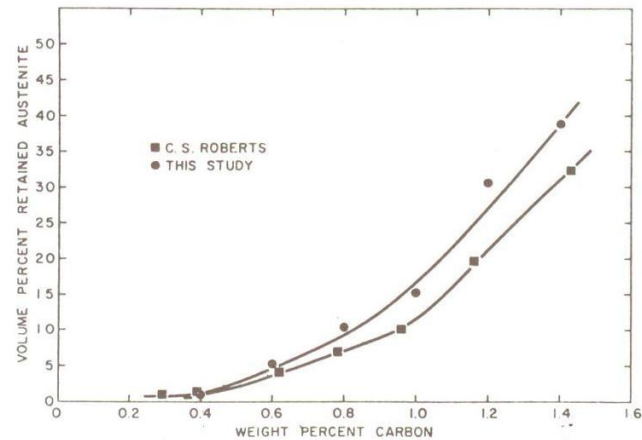


**FIGURE 1-30**

Retained austenite in quenched Fe-C alloys at room temperature as a function of carbon content. Note that the amount of retained austenite does not become significant until about 0.4% C. The Roberts data is from C. S. Roberts. *Trans. AIME* 197 (1953)203. [After A. R. Marder and G. Krauss, *Trans. ASM* 60(1967):651.]

repetition of laths of different but limited orientation through a whole domain of martensite. The formation of a lath domain is believed to be the result of a phase front that has propagated through a whole region of austenite matrix, resulting in the almost complete transformation of the parent austenite to martensite. As a result, only a small amount of retained austenite is present at room temperature in the low-carbon lath-type martensite (Fig. 1-30).

**TYPE II—PLATE-TYPE MARTENSITE.** The structure of martensite in high-carbon Fe-C alloys consists of needlelike plates of martensite often surrounded by large amounts of retained austenite. The plates are found to have irrational habit planes ranging from  $\{225\}$  to  $\{259\}$  as the carbon content increases. Above 1% C, the structure of Fe-C martensites is found to be exclusively plate martensite and retained austenite. In contrast to the low-carbon martensite, the plates found in the high-carbon martensites are formed independently on specific habit planes within the austenite and terminate or originate on one another. The plates in high-carbon martensite vary in size and have a fine structure of parallel *twins* which are of the  $\{112\}$  type (Fig. 1-31).

**MIXED LATH AND PLATE MARTENSITE.** There is a transition from lath- to plate-type martensite between 0.6 and 1.0% C in Fe-C alloys (Fig. 1-28). As the carbon content is increased, the size and frequency of the martensite plates



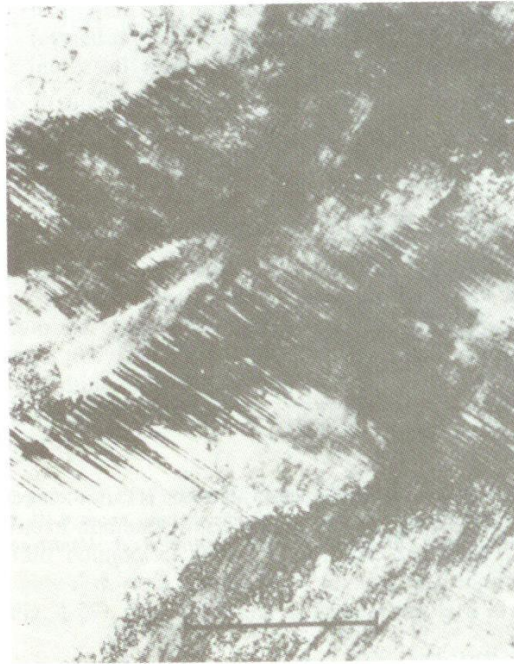


**FIGURE 1-31**  
Plate martensite showing fine transformation twins. [After M. Oka and C. M. Wayman, *Trans. ASM* 62(1969):370.]

increases and the amount of the lath martensite decreases. Kelly and Nutting<sup>1</sup> found that the factor that determined whether martensite would form as laths or plates was the transformation temperature at which a particular martensitic grain was formed. They believed that if the  $M_s$  temperature for an Fe-C alloy was below the critical transformation temperature, mostly plate-type martensite would be formed. The carbon content of an Fe-C alloy, since it controls the  $M_s$  temperature, would thus determine whether lath- or plate-type martensite would be formed. Therefore, there exists a range of temperatures for the formation of mixed lath and plate martensites, corresponding to a range of carbon contents from about 0.6 to 1.0 percent. This temperature band for Fe-C alloys is approximately 200 to 320°C.

### Mechanism of Formation of Martensite in Plain-Carbon Steels

**FEATURES.** At present the mechanism of formation of martensite in plain-carbon steels is not completely understood. The martensitic transformation in Fe-C alloys is very complicated. So while much research has been done on it, much more will be required in the future.

<sup>1</sup> P. M. Kelly and J. Nutting, *Proc. Roy Soc. London* A259(1960):45.

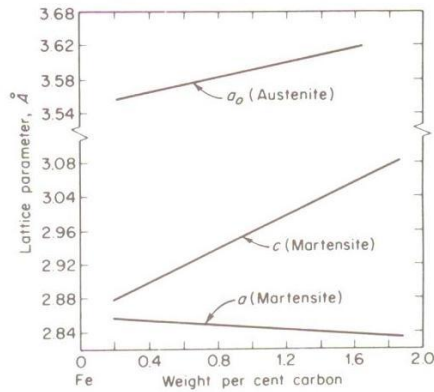


**FIGURE 1-32**

Variation of the lattice parameters of austenite and martensite as a function of carbon content. [After C. S. Roberts, *Trans. AIME* 197(1953):203, as presented in "Physical Metallurgy Principles," 2d ed., by R. E. Reed-Hill, ©1973 by Litton Educational Publishing, Inc., Reprinted by permission of D. Van Nostrand Co.]

The transformation of austenite to martensite occurs because below a critical temperature, designated the  $M_s$  temperature, martensite is the structurally stable state of the alloy and has a lower free energy. As stated before, the martensitic reaction in Fe-C alloys is diffusionless and therefore takes place without atom mixing. The martensitic reaction occurs with a cooperative rearrangement of the atoms, so that the relative displacement of the atoms is not more than the interatomic distance.

Certain features of the martensitic reaction are well established. Several of these are:

1. *The degree of tetragonality of the martensitic lattice increases as the carbon content increases.* Figure 1-32 shows how the  $c$  axis of a martensitic unit cell increases from 2.86 Å for the BCC structure to 3.08 Å for martensite with 1.8% C. Correspondingly, the  $a$  axis decreases from 2.86 to 2.83 Å in the same carbon range. This distortion of the BCC unit cell to a slightly BCT unit cell is a direct consequence of the carbon atoms straining the martensitic lattice into tetragonality.
2. *The change in morphology of Fe-C alloys with increasing carbon content is accompanied by a change in deformation mode from slip to twinning.* What causes the change is not completely understood. It is observed that, the higher the carbon concentration in the martensite, the greater is the tendency to form twinned plates. Lower  $M_s$  temperatures lead to increased twinning in martensitic structures. Increasing the strength of martensite and lowering the  $M_s$  temperature with more carbon solute favors twinning as the preferred shear mode.

**DEFORMATION MODES.** Explanations to account for slip and twinning have been proposed:

**Slip as a deformation mode in the formation of martensite.** To account for the experimentally observed high dislocation densities found in lath-type marten-

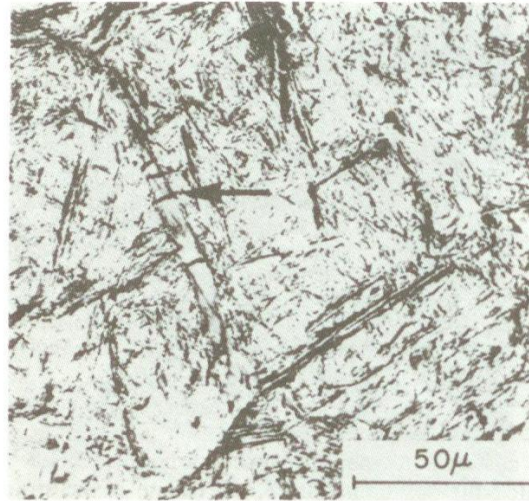


**FIGURE 1-33**  
Microstructure of a 0.93% C iron-carbon martensite specimen showing cracks in a martensite plate. Note the crack indicated by the arrow. (Etchant: sodium bisulfite.) [After A. R. Marder and G. Krauss, *Trans. ASM* 60(1967):651.]

site, Wasilewski<sup>1</sup> has proposed that *accommodation dislocations* are created, which are effectively sessile. These dislocations would form to relieve the very high levels of local strain energy formed by the rapid rate of formation of martensite. They would form more or less uniformly throughout single domains of martensite to accommodate the increased strain energy. As a result, domains with a high density of tangled accommodation dislocations would be formed, as is observed in lath martensite.

**Twinning as a deformation mode in the formation of martensite.** With higher carbon contents, the martensitic reaction becomes increasingly more difficult, as is indicated by the increase in amount of retained austenite (Fig. 1-30) under those conditions and by the effects of lowering the  $M_s$  temperature. As has been described, twinning becomes more and more the predominant mode of deformation as the carbon content increases.

As the transformation temperature is lowered, slip becomes increasingly more difficult. The important factor appears to be the relative magnitudes of the critical resolved shear stresses for twinning and slip at a given temperature and alloy composition. Wasilewski<sup>1</sup> suggests that twinning occurs as a means of preventing the failure of the lattice when sufficiently high strain energies accumulate locally. Thus a significant part of the elastic strain energy generated by the martensitic reaction at lower temperatures can be accommodated in the

<sup>1</sup> R. J. Wasilewski, *Metall. Trans.* 6A(1975):1405.



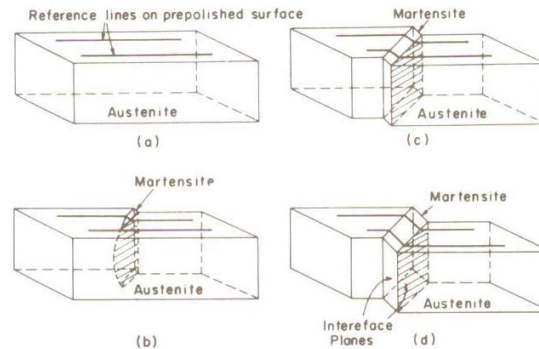


**FIGURE 1-34**  
Schematic representation of the martensite transformation in high-carbon iron-carbon alloys. [After M. Cohen, *Trans. AIME* 224(1962):638.]

twin/matrix coherent boundary, thereby lowering the average energy in the martensite. Even so, many times the elastic energy in the martensitic plates of the higher-carbon-containing Fe-C alloys cannot be accommodated by twinning, and cracking in the plates is observed, as shown by Marder and Krauss (Fig. 1-33).

The shape change which occurs during the formation of a martensitic plate in a high-carbon Fe-C alloy is shown schematically in Fig. 1-34. Deformation twinning has to occur in order for this type of a distortion to take place during the transformation of austenite to plate martensite. In this process, the surface of the crystal is tilted as shown in Fig. 1-35 for an Fe-1.86% C alloy. The relationship between the planes of the austenitic lattice and those of the martensite is not clear since many different relations have been proposed. However, the relationship usually cited for Fe-C alloys with 0.5 to 1.4% C is

$$(111)_\gamma \parallel (101)_\alpha \quad \text{with} \quad [1\bar{1}0]_\gamma \parallel [11\bar{1}]_\alpha$$

More research on this subject is necessary to clarify the situation.

**NUCLEATION AND GROWTH OF MARTENSITE.** It is generally accepted that martensitic embryos must form in the austenitic matrix at some high temperature and that the embryos must be activated to grow immediately when the  $M_s$  is reached. Favorable nucleation sites, according to Olson and Cohen,<sup>1</sup> are grain boundaries, incoherent twin boundaries, and inclusion particle interfaces. Also groups of dislocations can interact by plastic deformation to provide a suitable nucleation site. Martensite formed in one region of a sample can provide a combination of strain-induced nucleation and also provide elastic stresses to assist an existing nucleation site. This is called the *autocatalytic effect*.

The driving force for the growth of the martensite is the energy released in forming a lower-energy structure. The strain energy necessary to produce

<sup>1</sup> G. B. Olson and M. Cohen, *Metall. Trans.* 7A(1976):1905.



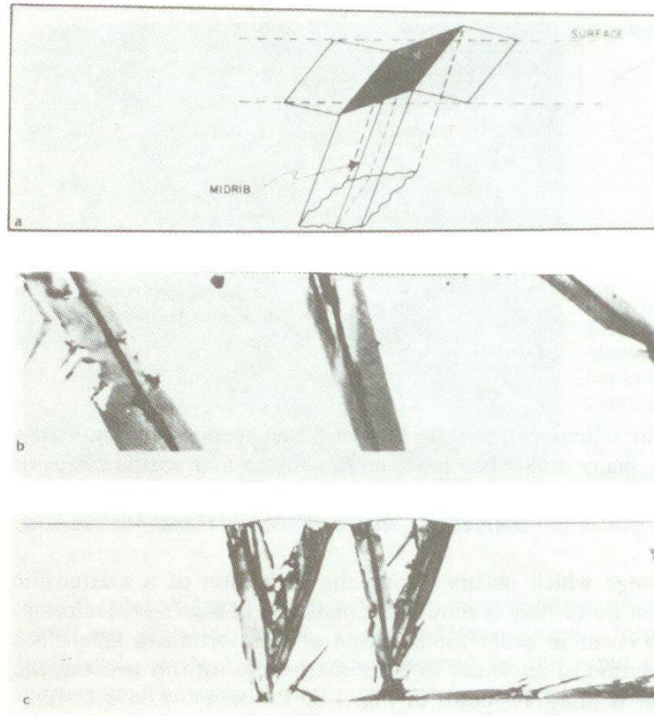


**FIGURE 1-35**

Shape deformation of plate martensite. (a) Schematic of shape change. (b) Shape of deformation in an Fe-1.86% C alloy. (c) Bulge in the austenite caused by martensite plate formation. (Etchant: nital:  $\times 1000$ .) [After G. Krauss and A. R. Marder, *Metall. Trans.* 2(1971):2343.]

martensitic laths or plates is more than compensated for by the volume free energy released by the formation of the martensitic phase. Observation shows that the austenite-martensite interface moves rapidly. After martensitic plates are nucleated, they grow rapidly until they strike another plate or grain boundary, and sometimes thicken slightly before stopping.

### Kinetics of Formation of Martensite in Plain-Carbon Steels

**RAPIDITY OF THE TRANSFORMATION.** Since the formation of martensite in Fe-C alloys is diffusionless, it only forms during the cooling process and not isothermally. The fraction of martensite that is formed depends only on the temperature to which it is cooled. Thus in the I-T diagram, horizontal lines are drawn to indicate percent martensite formed at a particular temperature. Such

a reaction, i.e., one that is only dependent on the temperature to which the martensite is quenched, is termed an *athermal transformation*. The percent martensite formed at a particular temperature does not depend on the cooling rate once a critical cooling rate is attained, but depends on the alloy composition and thermal and mechanical history.

The fact that the martensitic plates grow so rapidly must mean that there is little or no activation energy needed for their growth. The velocity of the growth of the plates in some cases approaches the speed of sound. The formation of the plates sometimes occurs by bursts such that the stresses produced by the formation of the initial plates catalyzes the nucleation of others.

**STABILIZATION.** Consider a sample of an austenitic plain-carbon steel which is being cooled rapidly to form martensite. If cooling is stopped for some time interval, say 1 s, at some temperature below the  $M_s$ , then the martensitic reaction will also stop, and the martensite is said to be *stabilized*. No further transformation of the austenite to martensite will occur even though there is sufficient free-energy difference for the reaction to continue. If the cooling of a stabilized steel is resumed, a certain amount of undercooling is necessary to start the austenite-to-martensite reaction again, and when it occurs it frequently begins with a burst. One theory to account for stabilization is that the carbon atoms diffuse to the dislocations in the martensite, thus preventing their further movement so that the reaction is stopped.

### Strength and Hardness of Martensite in Fe-C Alloys

The hardening produced in Fe-C martensites is directly related to their carbon contents. This relationship is clearly demonstrated in Fig. 1-36, which shows the hardness of fully hardened martensitic plain-carbon steels as a function of carbon content.

**LOW-CARBON MARTENSITES.** Four different strengthening effects of carbon in low-carbon martensites have been identified by Speich and Warlimont.<sup>1</sup> These are

1. Refinement of the martensite cell size with increasing carbon content
2. Segregation of carbon to the martensitic cell walls during the quench
3. Solid-solution hardening
4. Dispersion hardening due to precipitation of carbide during the quench

<sup>1</sup>G. R. Speich and H. Warlimont, *J. Iron Steel Inst.* 206(1968):385.

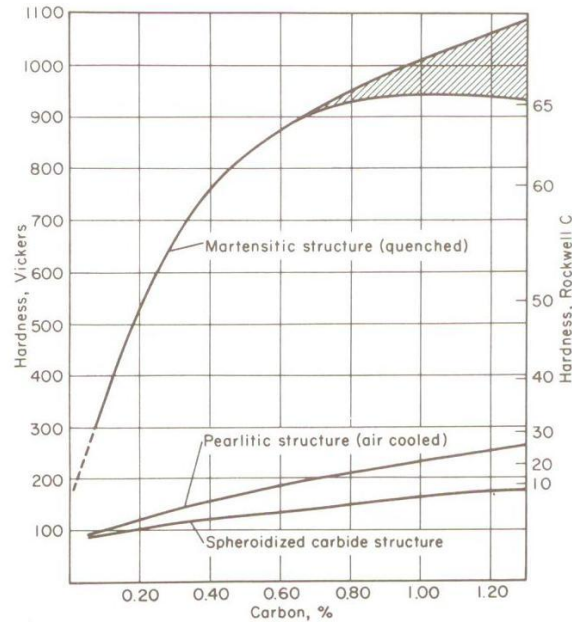


**FIGURE 1-36**

Approximate hardness of fully hardened martensitic plain-carbon steel as a function of carbon content. The cross-hatched region indicates some possible loss of hardness due to the formation of retained austenite, which is softer than martensite. (After E. C. Bain and H. W. Paxton, "Alloying Elements in Steel," 2d ed., American Society for Metals, 1966, p. 37.)

At low-carbon contents, lath martensite is formed which contains a high density of dislocations arranged in platelike cells. This cell structure is associated with an increase in strength in the low-carbon martensites. The stress required to move dislocations through dense dislocation networks and the finely spaced cell walls of the lath martensite would certainly be an important strengthening mechanism in low-carbon martensites. Items 2 to 4 above would also contribute in varying degrees to the strength of low-carbon martensites.

Figure 1-37 shows the net effect of all these mechanisms on the strength of low-carbon martensites in the 0.01 to 0.18% C range.

**HIGH-CARBON MARTENSITES.** With higher carbon contents in Fe-C alloys, solid-solution hardening becomes the dominant hardening mechanism, as is evidenced by the distortion of the BCC iron lattice into tetragonality. The increase in hardness can be correlated with the increased distortion of the iron

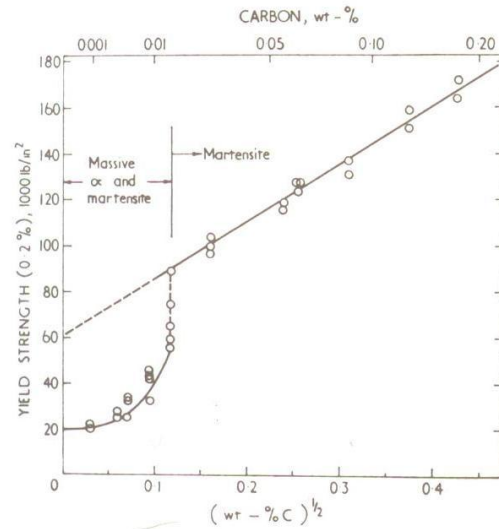


**FIGURE 1-37**  
Variation of the yield strength of low-carbon martensites with the square root of the carbon content. [After G. R. Speich and H. Warlimont, *J. Iron Steel Inst.* 206(1968):385.]

lattice. However, the introduction of numerous twinned interfaces in plate martensite would also be another hardening mechanism.

#### Example problem 1-1

- (a) 0.70% C hypoeutectoid plain-carbon steel is slowly cooled from 940°C to a temperature just slightly above 723°C.
- Calculate the weight percent austenite present in the steel.
  - Calculate the weight percent proeutectoid ferrite present in the steel.
- (b) 0.70% C hypoeutectoid plain-carbon steel is slowly cooled from 940°C to a temperature just slightly below 723°C.
- Calculate the weight percent proeutectoid ferrite present in the steel.
  - Calculate the weight percent eutectoid ferrite and weight percent eutectoid cementite present in the steel.

**Solution.** Referring to Fig. 1-7 and using tie lines:

$$(a) \text{ (i) Wt\% austenite} = \left( \frac{0.70 - 0.02}{0.80 - 0.02} \right) (100\%) = 87.2\% \blacktriangleleft$$

$$\text{(ii) Wt\% proeutectoid ferrite} = \left( \frac{0.80 - 0.70}{0.80 - 0.02} \right) (100\%) = 12.8\% \blacktriangleleft$$

- (b) (i) The weight percent proeutectoid ferrite present in the steel just below 723°C will be the same as that just above 723°C, which is 12.8% ◀

(ii) The weight percent total ferrite and cementite just below 723°C are

$$\text{Wt\% total ferrite} = \left( \frac{6.67 - 0.70}{6.67 - 0.02} \right) (100\%) = 89.8\%$$

$$\text{Wt\% total cementite} = \left( \frac{0.70 - 0.02}{6.67 - 0.02} \right) (100\%) = 10.2\%$$

$$\begin{aligned} \text{Wt\% eutectoid ferrite} &= \text{total ferrite} - \text{proeutectoid ferrite} \\ &= 89.8 - 12.8 = 77.0\% \blacktriangleleft \end{aligned}$$

$$\text{Wt\% eutectoid cementite} = \text{wt\% total cementite} = 10.2\% \blacktriangleleft$$

(No proeutectoid cementite was formed during cooling.)

**Example problem 1-2.** A hypoeutectoid plain-carbon steel which was slow-cooled from the austenitic region to room temperature contains 10.5 wt% eutectoid ferrite. Assuming no change in structure on cooling from just below the eutectoid temperature to room temperature, what is the carbon content of the steel?

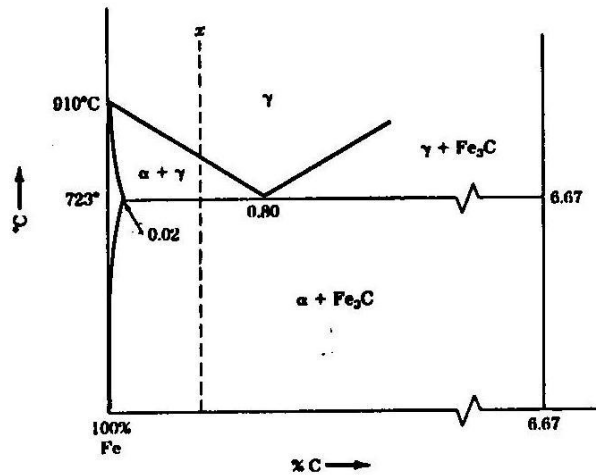


FIGURE EP1-2

**Solution.** Let  $x$  = the weight percent carbon of the hypoeutectoid steel. Now we can use the equation which relates the eutectoid ferrite to the total ferrite and the proeutectoid ferrite, which is

$$\text{Eutectoid ferrite} = \text{total ferrite} - \text{proeutectoid ferrite}$$

Using Fig. EP1-2 and the lever rule, we can make the equation

$$\frac{0.105}{\text{Eutectoid ferrite}} = \frac{6.67 - x}{6.67 - 0.02} - \frac{0.80 - x}{0.80 - 0.02} = \frac{6.67}{6.65} - \frac{x}{6.65} - \frac{0.80}{0.78} + \frac{x}{0.78}$$



$$\text{or} \quad 1.28x - 0.150x = 0.105 - 1.003 + 1.026 = 0.128$$

$$x = \frac{0.128}{1.13} = 0.113\% \text{ C} \blacktriangleleft$$

## PROBLEMS

- Describe the three allotropic forms of pure iron. Indicate how these are related to a cooling curve for pure iron.
- Draw the phase diagram for the Fe-Fe<sub>3</sub>C (metastable) alloy system and indicate the equilibrium critical temperatures.
- Describe the following solid phases which occur in the Fe-Fe<sub>3</sub>C diagram: (a)  $\alpha$  ferrite, (b) austenite, (c) cementite, and (d)  $\delta$  ferrite
- Write the invariant reactions which occur in the Fe-Fe<sub>3</sub>C diagram.
- Explain the meaning of the following designations on the Fe-Fe<sub>3</sub>C diagram when fast-cooling and -heating rates are involved:  $A_{c1}$ ,  $A_{r1}$ ,  $A_{c3}$ ,  $A_{r3}$ ,  $A_{c_{cm}}$ ,  $A_{r_{cm}}$ .
- Define eutectoid, hypoeutectoid, and hypereutectoid plain-carbon steels.
- Define the term "austenitizing."
- Distinguish between eutectoid and proeutectoid ferrite in the Fe-Fe<sub>3</sub>C diagram.
- Describe the structural changes which occur when a 0.6% plain-carbon steel is slowly cooled from the austenitic region.
- Repeat Problem 9 for a 1.1% hypereutectoid steel.
- Describe the procedure for making an isothermal transformation experiment for an eutectoid steel.
- Draw an isothermal transformation diagram for an eutectoid plain-carbon steel and indicate the cooling conditions necessary to form (a) pearlite, (b) bainite, and (c) martensite.
- Using a diagram describe the nucleation and growth of pearlite.
- Explain how the transformation of austenite to pearlite plotted as the percent pearlite transformed versus time leads to a sigmoidal curve.
- How does the rate of nucleation and growth in an eutectoid steel vary as a function of temperature? How can this relationship be explained qualitatively?
- How does the interlamellar spacing in pearlite vary with decreasing temperature in the isothermal transformation of an eutectoid steel?
- How does grain size affect the austenite-to-pearlite transformation of an eutectoid steel?
- How is the strength of pearlite affected by the interlamellar spacing?
- Describe the principal characteristics of the martensitic transformation in plain-carbon steels.
- Describe the morphological changes that occur in Fe-C martensites as the carbon content is increased from 0.2 to 1.2 percent.
- Describe the microstructure of lath Fe-C martensites.
- Describe the microstructure of plate Fe-C martensites.



23. What is believed to be the cause of the change from lath to plate martensite?
24. What explanation can be given for the change from slip to twinning deformation modes in martensite as the carbon content is increased?
25. What is the main cause of the cracking in martensitic plates in high-carbon Fe-C martensites?
26. What shape changes take place during the formation of martensitic plates in high-carbon Fe-C martensites?
27. Describe a possible mechanism for the nucleation and growth of a martensitic plate.
28. Describe what is meant by the term "athermal transformation." How can this term be applied to a martensitic transformation?
29. What is meant by the stabilization of martensite?
30. What are some of the strengthening mechanisms which are believed to be related to the strength of (a) low-carbon martensite and (b) high-carbon martensite?
31. Using the Fe-Fe<sub>3</sub>C metastable phase diagram, calculate the following for a slowly cooled 0.60% C hypoeutectoid steel:
  - (a) The weight percent austenite and proeutectoid ferrite just above 723°C
  - (b) The weight percent proeutectoid ferrite just below 723°C
  - (c) The weight percent cementite just below 723°C
  - (d) The weight percent eutectoid ferrite just below 723°C
32. (a) Using the Fe-Fe<sub>3</sub>C metastable phase diagram, calculate the following:
  - (i) The weight percent proeutectoid ferrite just below 723°C for a 0.75% hypoeutectoid steel
  - (ii) The weight percent proeutectoid cementite just below 723°C for a 0.85% hypereutectoid steel.
 (b) Why is the weight percent proeutectoid ferrite considerably larger than the weight percent proeutectoid cementite?
33. The stimulating autocatalytic effect of Fe-C plate martensitic formation on the further progression of the transformation has been attributed to a combination of strain-induced nucleation and an elastic stress assist of existing nucleation sites. Suggest a possible third contribution to this autocatalysis. [See G. B. Olson and Morris Cohen, "A General Mechanism of Martensitic Nucleation: Part II FCC, BCC, and Other Martensitic Transformations," *Metall. Trans.* 7A(1976):1905.]
34. During the formation of plate martensite in a Fe-1.39% C alloy, the increase in amount of plate martensite has been shown to be predominantly by the nucleation of new plates. By what other mode could the amount of plate martensite be increased as the temperature is decreased? [See G. Krauss and A. R. Marder, "Morphology of Martensite in Iron Alloys," *Metall. Trans.* 2(1971):2343.]
35. A 0.25% C hypoeutectoid plain-carbon steel is slowly cooled from about 950°C to a temperature just slightly above 723°C. Calculate the weight percent austenite and weight percent proeutectoid ferrite in this steel.
36. A 0.25% C hypoeutectoid plain-carbon steel is slowly cooled from 950°C to a temperature just slightly below 723°C.
  - (a) Calculate the weight percent proeutectoid ferrite in the steel.
  - (b) Calculate the weight percent eutectoid ferrite and weight percent eutectoid cementite in the steel.

37. A plain-carbon steel contains 90 wt% ferrite and 10 wt%  $\text{Fe}_3\text{C}$ . What is its average carbon content in weight percent?
38. A plain-carbon steel contains 58 wt% proeutectoid ferrite. What is its average carbon content in weight percent?
39. A plain-carbon steel contains 10.2 wt% eutectoid ferrite. What is its average carbon content?
40. A 1.05% C hypereutectoid plain-carbon steel is slowly cooled from 900°C to a temperature just slightly *above* 723°C. Calculate the weight percent proeutectoid cementite and weight percent austenite present in the steel.
41. A 1.05% C hypereutectoid plain-carbon steel is slowly cooled from 900°C to a temperature just slightly *below* 723°C.
  - (a) Calculate the weight percent proeutectoid cementite present in the steel.
  - (b) Calculate the weight percent eutectoid cementite and the weight percent eutectoid ferrite present in the steel.
42. If a hypereutectoid plain-carbon steel contains 6.4 wt% proeutectoid cementite, what is its average carbon content?
43. A hypereutectoid plain carbon steel contains 4.5 wt% proeutectoid  $\text{Fe}_3\text{C}$ . What is the average carbon content of the steel in weight percent?
44. A plain-carbon steel contains 19.5 proeutectoid ferrite. What is its average carbon content?
45. A 0.55% C hypoeutectoid plain-carbon steel is slowly cooled from 950°C to a temperature just slightly below 723°C.
  - (a) Calculate the weight percent proeutectoid ferrite in the steel.
  - (b) Calculate the weight percent eutectoid ferrite and eutectoid cementite in the steel.
46. A hypoeutectoid steel contains 35.1 wt% eutectoid ferrite. What is its average carbon content?
47. A hypoeutectoid steel contains 19.8 wt% eutectoid ferrite. What is its average carbon content?
48. If a thin sample of a eutectoid plain-carbon steel is hot-quenched from the austenitic region and held at 700°C until transformation is complete, what will be its microstructure?
49. If a thin sample of a eutectoid plain-carbon steel is water-quenched from the austenitic region to room temperature, what will be its microstructure?
50. Draw time-temperature cooling paths for a 1080 steel on an isothermal transformation diagram that will produce the following microstructures. Start with the steels in the austenitic condition at time = 0 and 850°C. (a) 100% martensite, (b) 50% martensite and 50% coarse pearlite, (c) 100% fine pearlite, (d) 50% martensite and 50% upper bainite, (e) 100% upper bainite, and (f) 100% lower bainite.
51. Thin pieces of 0.3-mm-thick hot-rolled strips of 1080 steel are heat-treated in the following ways. Use the IT diagram of Fig. 1-15 and other knowledge to determine the microstructure of the steel samples after each heat treatment.
  - (a) Heat 1 h at 860°C; water-quench.
  - (b) Heat 1 h at 860°C; water-quench; reheat 1 h at 350°C. What is the name of this heat treatment?

**44** STRUCTURE AND PROPERTIES OF ENGINEERING ALLOYS

- (c) Heat 1 h at 860°C; quench in molten salt bath at 700°C and hold 2 h; water-quench.
- (d) Heat 1 h at 860°C; quench in molten salt bath at 260°C and hold 1 min; air-cool. What is the name of this heat treatment?
- (e) Heat 1 h at 860°C; quench in molten salt bath at 350°C; hold 1 h; air-cool. What is the name of this heat treatment?
- (f) Heat 1 h at 860°C; water-quench; reheat 1 h at 700°C.

Patenting of steel wire, a technique invented back in the Eighteen Seventies in Britain, was kept a strict secret for decades. Keeping this technique "under wraps" enabled British firms to produce steel wire and fabricate steel-wire rope for a variety of applications.

The technology of patenting steel wire was first mastered in the USSR by S. S. Shteingerg [1] in 1922. Following analogous experiments, at the Belorussk steel wire factory, in joint work with engineers N. F. Andrianov and P. F. Zabalava; the secret of the method was discovered, and since that time steel wire production has undergone rapid development in our country.

The essentials of patenting involve an isothermal transformation of supercooled austenite in the first step, i.e., at 450-550°C. In order to ensure uniformity of the austenite and marked isochronal decay of the supercooled austenite at the temperature of the supercooling bath (fused salt or molten lead), the wire is heated to 150-200°C above the critical point (to 370°C to 320°C). In the supercooling bath the austenite decays rapidly to a quasieutectoid ferritic-carbide mixture of thin lamellar structure\* known as patenting sorbite. These ligatures of steel wire attach great importance to the grain size of the steel in thin lamellar patenting sorbite, on the assumption that a coarse grain must aid in the production of long wires in drawing processes, when total area reductions are considerable. It has turned out, in effect, that a highly dispersed, thin lamellar structure must form as a result of the high isothermality of the austenitic decay process in response to massive supercooling and to the formation of coarse grains.

The shape and size of the carbides is of great importance in cold drawing. The most highly favored form of carbide is the thin lamellar and uniform structure, and the least favored form is that of a network around pearlite grains. Rather an cementite (we prefer the term shell-type cementite) reveals cracks (fragments) leading to ruptures of the wire at the very outset of the drawing process. Carbides of pearlite in coarse lamellar form occupy an unfavorable position in terms of their effect on the ductility of the wire.

The presence of carbides of granular shape makes it possible to carry out various forms of cold plastic deformation (drawing, rolling, stamping, etc.). Granular carbides deform plastically to an extent at stage in the wire-drawing process, when area reductions are considerable.

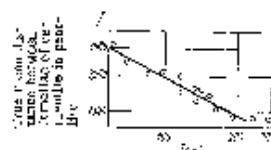


Fig. 1. Dependence of inter-lamellar distance in patenting sorbite on the temperature of isothermal decay of supercooled austenite.

The most striking ductility properties in drawing, given excellent strength characteristics, are exhibited by steel containing fine carbides in thin lamellar form (patenting sorbite). The degree of disperseness of the patenting sorbite (throughout the thickness of the carbide particles) depends on the temperature of the supercooling bath; the disperseness of the sorbite increases as the temperature of the bath (molten lead or fused salt) drops. Carbon steel with 0.15 to 0.55% C is usually subjected to patenting, and the temperature of the lead or salt bath is brought to 450-550°C.

\* Given the fluctuations of microsegregation structures of the early twenties, S. S. Shteingerg was of the opinion that cementite had a globular shape in patented wire [1].